INTERNATIONAL STANDARD

ISO 17201-3

Second edition
2019-01

Acoustics — Noise from shooting ranges —

Part 3:
Sound propagation calculations

Acoustique — Bruit des stands de tir —

Partie 3: Calcul de la propagation du son

Reference number
ISO 17201-3:2019(E)

ISO copyright office
CP 401 • Ch. de Blandonnet 8
CH-1214 Vernier, Geneva
Phone: +41 22 749 01 11
Fax: +41 22 749 09 47
Email: copyright@iso.org
Website: www.iso.org

Published in Switzerland

Contents

Page

Foreword .... **iv**
Introduction .... **v**
1 Scope **1**
2 Normative references **1**
3 Terms and definitions **1**
4 Source modelling **2**
4.1 General 2
4.2 Muzzle blast 2
4.2.1 Background 2
4.2.2 Free-field situation 3
4.2.3 Non-free-field situation 3
4.3 Projectile sound 6
5 Propagation calculation **6**
5.1 General 6
5.2 Application of ISO 9613-2 for free-field situations 6
5.3 Application of ISO 9613-2 for non-free-field situations 8
5.4 Sophisticated models 8
6 Conversion of sound exposure levels **9**
7 Uncertainties **10**
Annex A (normative) **Benchmark cases for shooting sheds with baffles** **11**
Annex B (informative) **Sophisticated modelling approaches** **27**
Annex C (informative) **Modelling of shooting scenarios — Examples of shooting ranges** **36**
Annex D (informative) **Uncertainty** **54**
Bibliography **58**

Foreword

ISO (the International Organization for Standardization) is a worldwide federation of national standards bodies (ISO member bodies). The work of preparing International Standards is normally carried out through ISO technical committees. Each member body interested in a subject for which a technical committee has been established has the right to be represented on that committee. International organizations, governmental and non-governmental, in liaison with ISO, also take part in the work. ISO collaborates closely with the International Electrotechnical Commission (IEC) on all matters of electrotechnical standardization.

The procedures used to develop this document and those intended for its further maintenance are described in the ISO/IEC Directives, Part 1. In particular the different approval criteria needed for the different types of ISO documents should be noted. This document was drafted in accordance with the editorial rules of the ISO/IEC Directives, Part 2 (see www.iso.org/directives).

Attention is drawn to the possibility that some of the elements of this document may be the subject of patent rights. ISO shall not be held responsible for identifying any or all such patent rights. Details of any patent rights identified during the development of the document will be in the Introduction and/or on the ISO list of patent declarations received (see www.iso.org/patents).

Any trade name used in this document is information given for the convenience of users and does not constitute an endorsement.

For an explanation on the meaning of ISO specific terms and expressions related to conformity assessment, as well as information about ISO's adherence to the World Trade Organization (WTO) principles in the Technical Barriers to Trade (TBT) see the following URL: www.iso.org/iso/foreword.html.

This document was prepared by ISO/TC 43, *Acoustics*, Subcommittee SC 1, *Noise*.

This second edition cancels and replaces the first edition (ISO 17201-3:2010), of which it constitutes a minor revision. The changes compared to the previous edition are as follows:

— Formulae (B.1) and (B.3) have been corrected by insertion of F_0.

— Minor corrections have been made in Annex C.

A list of all parts in the ISO 17201 series can be found on the ISO website.

Any feedback or questions on this document should be directed to the user's national standards body. A complete listing of these bodies can be found at www.iso.org/members.html.

Introduction

The initiative to prepare a standard on impulse noise from shooting ranges was taken by AFEMS, the Association of European Manufacturers of Sporting Ammunition, in April 1996 by the submission of a formal proposal to CEN. After consultation in CEN in 1998, CEN/TC 211, *Acoustics* asked ISO/TC 43, *Acoustics*, Subcommittee SC 1, *Noise* to prepare ISO 17201 (all parts).

This document provides guidance for sound propagation calculation of shooting sound from shooting ranges. If calculation procedures are not implied or specified by local or national guidelines, rules and regulations, and if a more sophisticated propagation model is not available, then ISO 9613-2 may be applied, provided that the recommendations in this document are observed.

The source energy of muzzle blast is typically measured or calculated for free-field conditions and often exhibits strong directivity. In many cases, firearms are fired within a shooting range which has structures such as firing sheds, walls or safety barriers. Guns, particularly shotguns, are sometimes fired in many directions, e.g. in trap and skeet where the shooting direction is dictated by the flight path of the clay target. This document recommends ways in which source data can be adapted for use with ISO 9613-2 to obtain a general survey for the sound exposure levels to be expected in the neighbourhood around shooting ranges.

Acoustics — Noise from shooting ranges —

Part 3: Sound propagation calculations

1 Scope

This document specifies methods of predicting the sound exposure level of shooting sound for a single shot at a given reception point. Guidelines are given to calculate other acoustic indices from the sound exposure level. The prediction is based on the angular source energy distribution of the muzzle blast as defined in ISO 17201-1 or calculated using values from ISO 17201-2.

This document applies to weapons with calibres of less than 20 mm or explosive charges of less than 50 g TNT equivalent, at distances where peak pressures, including the contribution from projectile sound, are less than 1 kPa (154 dB).

NOTE National or other regulations, which could be more stringent, can apply.

2 Normative references

The following documents are referred to in the text in such a way that some or all of their content constitutes requirements of this document. For dated references, only the edition cited applies. For undated references, the latest edition of the referenced document (including any amendments) applies.

ISO 9613-2:1996, *Acoustics — Attenuation of sound during propagation outdoors — Part 2: General method of calculation*

ISO 17201-1:2018, *Acoustics — Noise from shooting ranges — Part 1: Determination of muzzle blast by measurement*

ISO/IEC Guide 98-3[1)], *Uncertainty of measurement — Part 3: Guide to the expression of uncertainty in measurement (GUM:1995)*

3 Terms and definitions

For the purposes of this document, the following terms and definitions apply.

ISO and IEC maintain terminological databases for use in standardization at the following addresses:

— ISO Online browsing platform: available at https://www.iso.org/obp

— IEC Electropedia: available at http://www.electropedia.org/

3.1
substitute source
substitute for a sound source and its *firing shed* (3.4) by a model source without a firing shed positioned in the centre of the opening of the firing shed to represent the emission in the direction of a reception point

3.2
safety barrier
<shooting ranges> barrier that is intended to stop projectiles leaving the range

1) ISO/IEC Guide 98-3 is published as a reissue of the Guide to the expression of uncertainty in measurement (GUM), 1995.

3.3
safety baffle
<shooting ranges> overhead barrier that is intended to stop projectiles leaving the range

3.4
firing shed
structure constructed to protect the shooters and their equipment from precipitation and wind, having an opening that allows shooting at a target located on open ground

3.5
shooting range
enclosed arrangement of *firing positions* (3.7) and matching targets which, depending on the design, may include such features as a *firing shed* (3.4), *safety barriers* (3.2), *safety baffles* (3.3), and unsafe areas

3.6
shooting facility
organizational entity consisting of one or more *shooting ranges* (3.5), and associated buildings and infrastructure

3.7
firing position
position of the shooter within a *shooting range* (3.5)

3.8
impact sound
sound produced by the projectile hitting the target

3.9
diffraction point
point on top of a barrier which provides the shortest path length for the sound travelling over the barrier to the reception point

4 Source modelling

4.1 General

The basic quantities to be used are the angular source energy distribution, $S_q(\alpha)$, and angular source energy distribution level, $L_q(\alpha)$, as defined in ISO 17201-1. The angle between the line of fire and the line from the muzzle to the reception point is designated by α. If the gun is fired in a free-field situation, $S_q(\alpha)$ can be used to describe the muzzle blast. For rifle shots, projectile sound has to be included (see 4.3). Substitute sources can be used for shed situations and for the incorporation of reflection and diffraction to calculate the reception levels as if it was a free-field situation. Impact sound caused by the projectile hitting the target can usually be neglected. This document does not apply to projectiles containing a charge which is detonated at the target.

4.2 Muzzle blast

4.2.1 Background

For the non-free-field situation (such as a shed with one opening), the propagation model of ISO 9613-2 is insufficient, and more complex propagation models and calculation procedures are needed. Annex A provides a benchmark case and a demonstration of how sophisticated sound propagation approximations (see Annex B) may be used to describe the sound emitted from such a range, based on the free-field data of the angular source energy distribution levels. The sound emission is then expressed by the angular source energy distribution level of a substitute source positioned at a representative position in front or above the firing shed. All further calculations of the sound pressure level are carried out as specified in Clause 5 by a point source with directivity independent from the range, which may be formed by a shed, baffles and side walls, etc.

4.2.2 Free-field situation

If the weapon under consideration is used outside a firing shed or similar structure, use the angular source energy distribution level, $L_q(\alpha)$, of the specific weapon/ammunition combination directly. If a shot is fired with a reflecting surface near the shooter, take the reflection into account. The directivity has to be adjusted accordingly. If the gun can be fired in varying horizontal and vertical directions, account for these directions separately. Examples of free-field situations are described in Annex C.

4.2.3 Non-free-field situation

4.2.3.1 Shooting shed

In this case, the shot is fired in a shed (see for example Annex B). Part of the energy radiated due to the muzzle blast is absorbed by the walls and the ground. If baffles and side walls are present, take the reflections from the ground, side walls and baffles into account (see Annex A). An absorbing ceiling within the shed can be considered to be state of the art. The remaining energy is emitted through the opening of the shed. Therefore, free-field data shall not be used directly. If no absorption occurs within the shed and at the baffles, the benchmark case is not a suitable model to describe the emitted sound energy.

Figure 1 depicts a shed with the side walls and safety overhead baffles.

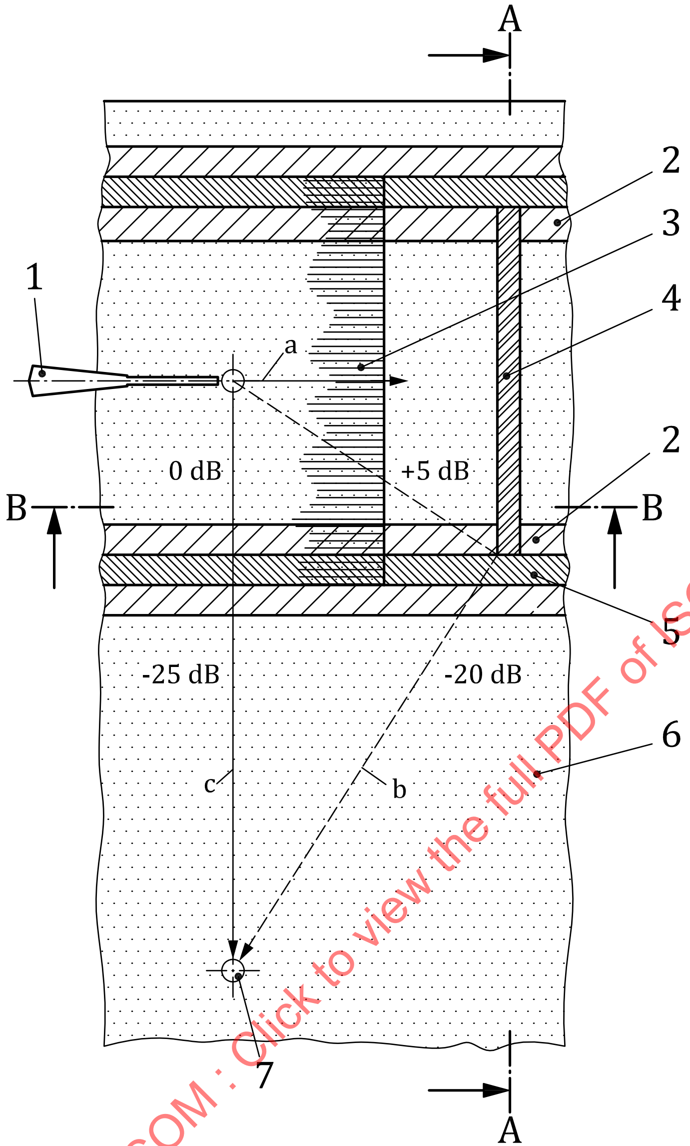

a) Top view

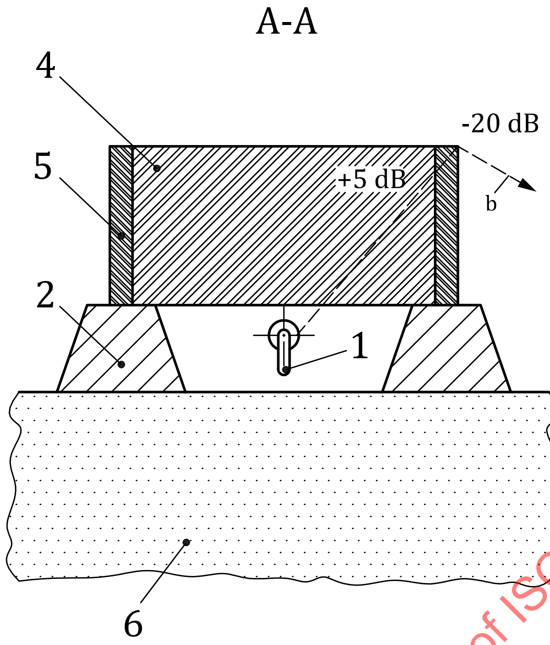

b) View in shooting direction

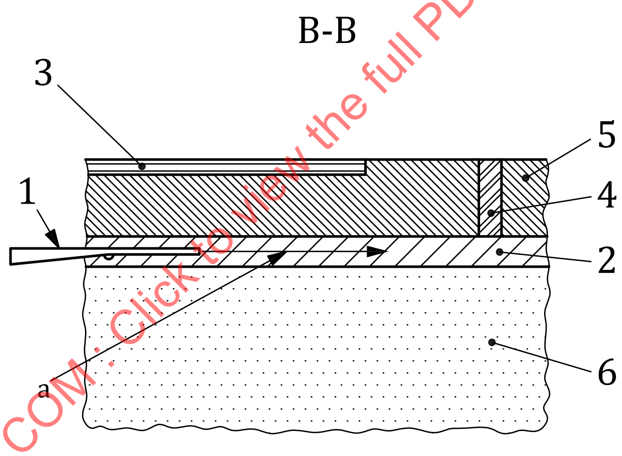

c) Side view

Key

1	gun/rifle	7	reception point
2	side berm	a	Shooting direction.
3	roof	b	Diffracted sound.
4	safety baffle	c	Shielded sound.
5	barrier		
6	ground		

Figure 1 — Shooting shed situation and illustration of diffraction effects on the propagation path

4.2.3.2 More complex situations

For more complex situations consisting of different shooting facilities, such as a trap and skeet range together with rifle ranges for large and small calibres, a larger number of sources and substitute sources sometimes have to be included to adequately model the situation. These sources are considered incoherent. However, reflections are considered to be coherent, when at the reception point the time delay between the muzzle blast and its reflections is less than 3 ms. Then, they shall be modelled as one substitute source. If the prediction focuses on F-time-weighted levels, substitute sources can combine multiple sound paths that have time delays within a time span less than (125/2) ms.

NOTE 62,5 ms is half the exponential time constant for time-weighting F (125 ms) as specified in IEC 61672-1:2013, 5.8.1.

4.3 Projectile sound

Modelling of projectile sound is described in ISO 17201-2 and ISO 17201-4. ISO 17201-4 also gives guidelines for the calculation of the propagation of projectile sound, as far as it deviates from the propagation of other sound. This means that for the attenuation for projectile sound, A_{excess}, ISO 9613-2 can also be used. The other attenuation parameters such as geometrical divergence, air absorption and non-linear attenuation are specified in ISO 17201-4. In free-field situations, especially in front of the weapon when the distance to the trajectory is short, projectile sound can be a relevant source for the sound exposure level of shooting sound. If a shot is fired in a shooting range, projectile sound is in general of minor importance in the estimation of the sound exposure level at a reception point. However, if measures are taken to reduce the sound emission of the muzzle blast, projectile sound can then become a dominant factor.

5 Propagation calculation

5.1 General

The propagation calculation may be performed using ray-tracing or more sophisticated models, which take specific weather conditions into account. To calculate a long-term L_{eq}, the results are weighted with respect to the frequency of occurrence of weather conditions pertinent to the time periods of interest during which the shooting range is operated.

5.2 Application of ISO 9613-2 for free-field situations

ISO 9613-2 neither applies to shooting sound nor accounts for changes in sound pressure time history during propagation. It therefore cannot yield results for time-weighted metrics such as L_{Fmax} (see Clause 6). ISO 9613-2 does not adequately account for meteorological effects on sound propagation over distances greater than 1 km. Furthermore, the use of ISO 9613-2 is not recommended if the spectrum at the reception point is dominated by frequencies below 100 Hz.

However, ISO 9613-2 may be applied to model propagation of shooting sound if modifications are introduced.

The sound power level and the directivity have to be substituted by the angular source energy distribution level and the ambient level by the resulting sound exposure level, $L_E(f)$, at the reception point of one specific shot under favourable sound propagation conditions.

The sound exposure level for one shot fired is obtained by:

$$L_E\left(f\right)=L_q\left(\alpha,f\right)-A_{\text{div}}\left(r\right)+11\,\text{dB}-A_{\text{atm}}\left(r,f\right)-A_{\text{bar}}\left(r,f\right)-A_{\text{gr}}\left(r,f\right)-A_{\text{z}}\left(r,f\right)-A_{\text{misc}}\left(r,f\right) \quad (1)$$

where

$L_q(\alpha,f)$ is the angular source energy distribution level, in decibels, of the weapon ammunition combination under consideration;

r is the distance, in metres, from the source or substitute source $\text{P}(x_0, y_0, z_0)$ to the reception point $\text{P}(x, y, z)$;

α is the angle between the line of fire and the line from the source to the reception point $\text{P}(x, y, z)$, provided that the latter line does not interfere with a barrier;

f is the centre frequency, in hertz, of any frequency band;

A_{div} is a correction, in decibels, for the geometric spread;

A_{atm} is the air absorption, in decibels, according to ISO 9613-1;

A_{bar} is the shielding by barrier, in decibels, according to ISO 9613-2;

A_{gr} is the ground effect, in decibels, according to ISO 9613-2;

A_z is a correction for non-standard meteorological conditions [see ISO 3741[2], ISO 3745[3], ISO 9614-3[4], and ISO 17201-1:2018, Formula (11)];

A_{misc} is a correction, in decibels, for miscellaneous other effects according to ISO 9613-2.

Concerning α, if the sound is shielded by a barrier, separate calculations for each point of diffraction are necessary. The angle, α, used to obtain $L_q(\alpha, f)$ is the angle between the line of fire and the line from the source point to the point of diffraction under consideration. This approach deviates from ISO 9613-2.

The insertion loss, A_{bar}, is related to sound exposure level in the direction of the point of diffraction (see example in Annex C) for the same distance between the reception point and the source point (see Reference [11]).

To include the ground effect and determine A_{gr}, ISO 9613-2:1996, 7.3.1 can be used. ISO 9613-2:1996, 7.3.2 can also be used, in which case an additional term D_Ω needs to be added to $L_q(\alpha, f)$. D_Ω can be determined by using ISO 9613-2:1996, Formula (11), or it can be set to 3 dB.

The calculation of $L_q(x, y, z, f)$ for a shed opening is specified in 5.3.

The long-term sound exposure level is obtained by:

$$L_{E,\text{long term}} = L_E - C_{\text{met}} \tag{2}$$

The way to obtain C_{met} depends strongly on the definition of the weather condition for which the sound exposure level, $L_E(f)$, is to be calculated. If the long-term L_{eq} is needed, take the long-term weather conditions at the site into account. If such information is not available, C_{met} for the long term $L_{A,eq}$ can be determined according to ISO 9613-2:1996, Formula (22), using C_0 = 5 dB. By application of ray tracing models and long-term statistics of wind direction, wind speed and atmospheric stability, a more accurate value for long-term levels can be obtained (see References [12], [13]).

NOTE The value 5 dB for C_0 results from the assumption that favourable sound propagation conditions occur for one third of the time.

If ISO 9613-2 is applied, the following limitations are observed:

— For longer distances, ISO 9613-2 has the tendency to overestimate the long-term sound exposure level, $L_{E,\text{long term}}$, during daytime (Reference [14]).

— For downwind conditions, the effect of screens can be overestimated as a consequence of the induced air flow at the top of the screen (Reference [15]).

— During daytime, the barrier attenuation tends to be higher compared to the value obtained by ISO 9613-2 (Reference [16]).

— ISO 9613-2 does not consider diffraction apart from shielding. However, diffracted sound from safety baffles for example (see Figure 1) can produce a major contribution at the reception point.

Scattering is only approximately taken into account. That effect can be an important contribution to the overall level at a reception point for situations in which the sound sources are well shielded.

5.3 Application of ISO 9613-2 for non-free-field situations

For calculation of the sound immission in a non-free-field situation, more sophisticated sound propagation models are needed (see 5.4). These model calculations are usually very time consuming. Even if the distance between the shooting range and the reception point is not more than a few hundred metres, the calculation over all frequencies takes too long to be used for noise mapping.

Therefore the concept of the substitute source is introduced to allow the use of generally available software to calculate noise maps. A sophisticated model is used to calculate the sound exposure level, $L_E(f)$, at some immission-relevant reception points, P(x, y, z), which are far enough from the shed to allow the substitution of the original source and its direct surroundings by a point source with directivity characteristics. The distance between the range and such a reception point should at least be twice the largest dimension of the range. The position of the substitute source with the angular source energy distribution level, $L_{q,S}(x, y, z, f)$, for this reception site and other reception sites is chosen to be in the middle of the opening through which most of the sound energy travels. For a simple shed without barriers and baffles, the source point is chosen to be in the middle of the shed opening. For ranges with a shed and barriers and baffles, the position is chosen in the centre of the first opening (see Figure B.1, point P).

The calculated levels can also be chosen on a circle and the angular source energy distribution level can then be calculated according to the procedures specified for measurement in ISO 17201-1.

The angular source energy distribution level of the substitute source, $L_{q,S}(\alpha, f)$, is calculated from the exposure level using Formula (3).

$$L_{q,S}(\alpha, f) = L_E(x, y, z, f) - 11\,\text{dB} + A_{\text{div}}(r) \tag{3}$$

where

$L_E\,(x, y, z, f)$ is the sound exposure level, expressed in decibels, for frequency f at point P(x, y, z) obtained by boundary element method (BEM) or similar (see Annex B);

$A_{\text{div}}\,(r)$ is the correction, expressed in decibels, for geometrical divergence between the assumed source position and point P(x, y, z);

r is the distance, in metres, between the chosen substitute source position and P(x, y, z).

In this model, the substitute source replaces the original source and its direct surroundings. If only the direction of α is of interest, Formula (1) can be applied directly. If the directivity is needed, as for example in a noise map, use the process specified in ISO 17201-1. A_{atm}, A_{bar}, A_{gr}, A_{misc} are excluded from the calculation of $L_{q,S}(\alpha)$. Only take into account barrier effects, etc. for those barriers which are not included in the calculation using the sophisticated model.

Figure 1 shows a typical shooting shed with the overhead baffles and side walls. In Annex A, the sound exposure level for a gun fired in such a shed is given. This has been calculated with the BEM over hard ground for a number of heights and positions in the surrounding. In the benchmark case, the ground reflection has been included; A_{atm}, A_{bar} and A_{misc} have been assumed to be zero.

For existing situations, it is recommended that the chosen sophisticated model be verified by measurement of the sound exposure level at the reception point, provided that the actual propagation conditions during the measurements are well defined. For propagation calculation outside the shed, the ground reflection has been included. Ensure that the same surface type is used for any sophisticated model as well as for the application of ISO 9613-2.

5.4 Sophisticated models

For the non-free-field situation, more sophisticated calculation models – compared to ISO 9613-2 – are needed. BEMs, ray-tracing models, wave models or combinations should be used in which reflection, diffraction and scattering can be taken into account in more detail (see Annex A, Annex B and References [17], [18], [19], [20]).

A benchmark case is given in Annex A for a shed as depicted in Figure A.1. This case has been calculated using BEM.

If other models or approximations are used such as

— Kirchhoff-approximation (see B.2),

— ray tracing models (see B.3),

ensure that the sound exposure levels of the benchmark case according to Annex A at 100 Hz and 200 Hz are reproduced by the levels of the sophisticated model without significant deviations. For distances twice as large, the model levels should not be greater than +5 dB and not less than −1 dB compared to the benchmark case:

$$L_{\text{benchmark}} + 5\ \text{dB} > L_{\text{model}} > L_{\text{benchmark}} - 1\ \text{dB} \tag{4}$$

with a probability of less than 5 %.

6 Conversion of sound exposure levels

Sound exposure level, L_E, is a widely used metric for sound from small arms. However, a number of metrics in legal codes or regulations generally used to describe small arms noise are based on the maximum level for a specific time weighting. An estimate of these metrics can be obtained from the relationships:

$$L_{\text{Smax}} \approx L_E \tag{5}$$

$$L_{\text{Fmax}} \leq L_E + 9{,}0\ \text{dB} \tag{6}$$

$$L_{\text{Imax}} \leq L_E + 14{,}6\ \text{dB} \tag{7}$$

$$L_{\text{Imax}} \leq L_{\text{Fmax}} + 5{,}6\ \text{dB} \tag{8}$$

where

L_{Smax} is the highest S-time-weighted sound pressure level within a stated time interval, expressed in decibels;

L_{Fmax} is the highest F-time-weighted sound pressure level within a stated time interval, expressed in decibels;

L_{Imax} is the highest I-time-weighted sound pressure level within a stated time interval, expressed in decibels.

The equal sign is valid if the event duration is less than 10 % of the time constant of exponential time weighting, τ (S: τ =1 s, F: τ =0,125 s, I: the onset time constant τ =0,035 s differs from the decay time constant τ = 1,5 s), which is the case close to the source and if no reflections occur.

For increasing distances, the duration of the time signal increases, e.g. as a consequence of ground reflections. The sound pressure time history of the signal including its reflections needs to be calculated to ensure the proper evaluation of the above metrics. If sufficient information is not available, L_{Imax} may, according to Reference [21], be approximated by:

$$L_{\mathrm{I,max}} = \begin{cases} L_E + 14{,}6\,\mathrm{dB} - 0{,}003\, r / R_0\ \mathrm{dB} & \text{for} \quad r < 2\,000\ \mathrm{m} \\ L_E + 8{,}6\,\mathrm{dB} & \text{for} \quad r \geq 2\,000\ \mathrm{m} \end{cases} \tag{9}$$

where

r is the distance, in metres, between the substitute source and the reception point P(x, y, z);

R_0 is 1 m.

The relations are valid for single shots when the time lapse between successive shots is greater than the time constant.

7 Uncertainties

The uncertainty of the one-third-octave-band spectrum of the sound exposure level of the muzzle blast determined in accordance with this document shall be evaluated, preferably in conformity with ISO/IEC Guide 98-3.

The uncertainties arise from a number of causes:

— the angular source energy distribution level (see ISO 17201-1 for situations in which that level is determined by measurements or ISO 17201-2 when that level is estimated based on the chemical energy of the propellant);

— the modelling of an actual complex source situation into a substitute source or a number of substitute sources;

— the modelling of the actual situation by simplification of the propagation-influencing objects (complex structures modelled by cubes, uneven terrain modelled by flat terrain, etc.);

— the position of the sound source with respect to the propagation influencing objects and the actual shooting direction;

— the sound propagation model used.

If, instead of the sound exposure level, another metric is used for the evaluation of shooting sound, additional uncertainties arise from the estimation of these metrics from the sound exposure level.

If the prognosis is done on the basis of the acoustical energy of all shots over a certain time period, uncertainties also arise with respect to the actual number of shots fired and the actual weapon and ammunition combinations.

The expanded uncertainty together with the corresponding coverage factor shall be stated for a coverage probability of 95 % as defined in ISO/IEC Guide 98-3.

Guidance on how to evaluate and express the uncertainty is given in Annex D.

Annex A
(normative)

Benchmark cases for shooting sheds with baffles

A.1 General

The benchmark case is based on the numerical solution of the Helmholtz-Kirchhoff wave equation using BEM (see Reference [22]). For simplicity, a small shooting shed with three overhead safety baffles is used, projectile sound is neglected and the directivity is assumed to be uniform.

A.2 Benchmark case

A.2.1 Model shed

Figure A.1 shows the geometry of the shed modelled. This consists of a rectangular box, with a semi-open ceiling with baffles. The geometry is approximately that of a typical 25 m long shooting shed used in the Netherlands; however, in the benchmark case, the length has been reduced to test for the proper function of the solution for longer wavelengths. A *xyz*-co-ordinate system is used, with the *x*-axis along the shooting direction. Dimensions are indicated in Figure A.1. The baffles are 2 m high, so the space between the ground and the baffles is also 2 m high.

All walls and the ceiling have a finite thickness of about one-sixth of a wavelength (for computational reasons). For a frequency of 100 Hz, the thickness is 0,5 m; for a frequency of 200 Hz, the thickness is 0,25 m. The source is a monopole source located on the ground, at position P(−3 m, 0 m, 0 m). All inner surfaces are acoustically absorbing (shown in Figure A.1), except for the ground surface and the baffles, which are acoustically rigid (shown in Figure A.1). Outer surfaces are all rigid. For the absorbing surfaces, a normalized impedance of unity was assumed (normalized to the impedance of air).

Dimensions in metres

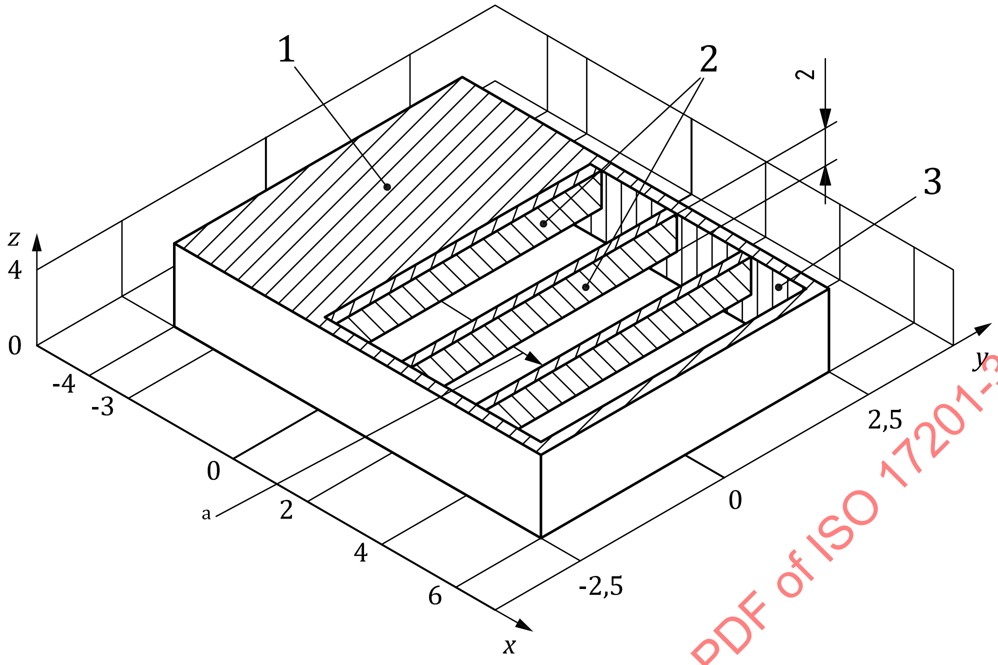

Key

1 roof

2 overhead safety barrier

3 side wall

a Shooting direction.

Figure A.1 — Geometry of the benchmark model shooting range

A.2.2 Computational method

The BEM in acoustics (see Reference [22]) is a numerical technique for solving the Kirchhoff-Helmholtz integral equation. The basic idea of the method is that the Kirchhoff-Helmholtz integral is approximated numerically by representing all solid boundaries in the system by a finite number of surface elements. The elements have linear dimensions of the order of one sixth of a wavelength or smaller. The calculations are performed with an implementation of BEM which neglects the variation of the acoustic pressure within a single surface element. The rigid ground surface is treated as a plane of symmetry in this case, by including an image system below the ground surface.

A.3 Results

Figure A.2 and Figure A.3 show BEM results at two frequencies (100 Hz and 200 Hz, respectively) and three reception heights (2 m, 5 m and 8 m), in a rectangular area of 160 m × 160 m around the shooting range. The colour represents the relative sound pressure level, i.e. the level *with* the shooting range minus level *without* the shooting range. In other words, the relative sound pressure level is equal to minus the insertion loss of the shooting range. Thus, the relative sound pressure level is *low* and the insertion loss is *high* in shadow regions.

Values of the insertion loss at a grid with spacing 10 m are given in Tables A.1 to A.6.

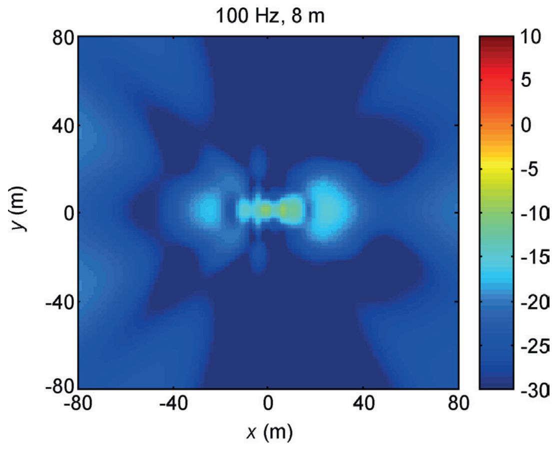

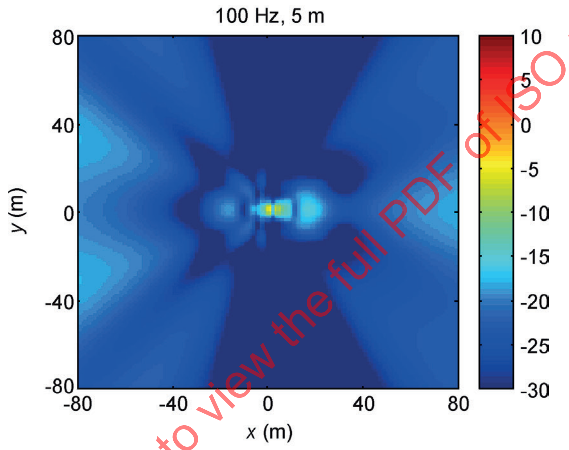

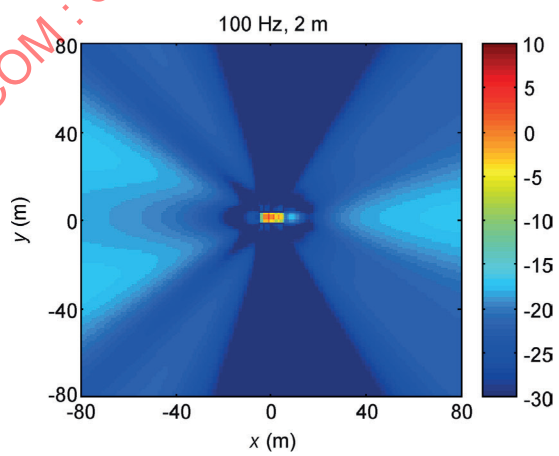

Figure A.2 — Relative sound pressure level, in dB, at frequency 100 Hz, for three reception heights (2 m, 5 m and 8 m)

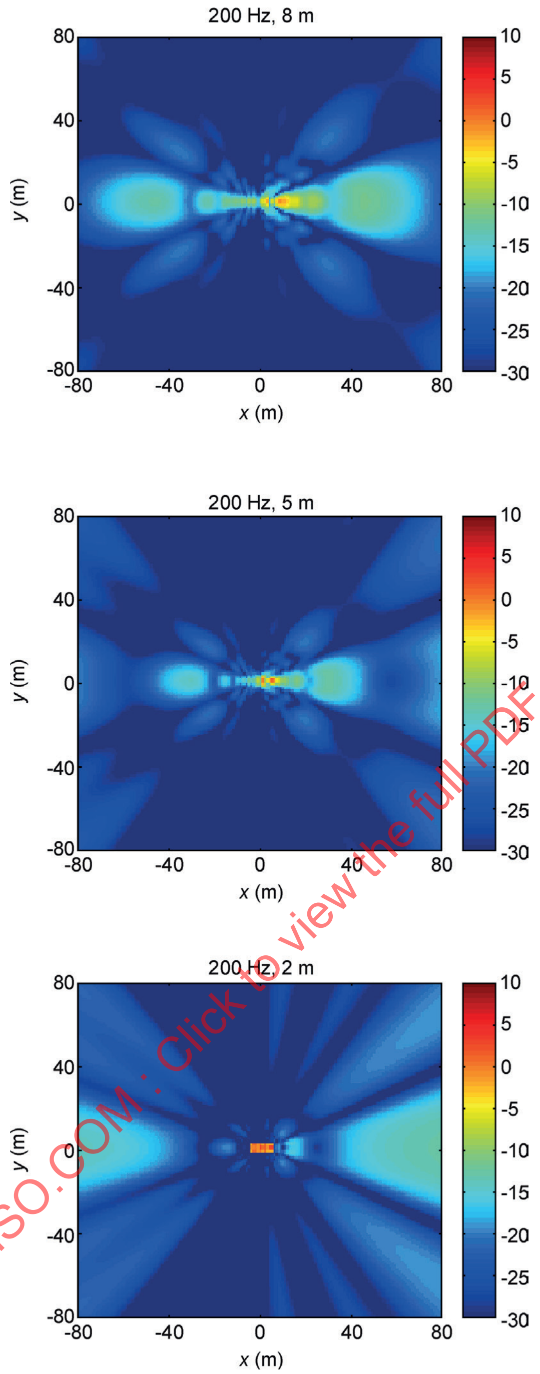

Figure A.3 — Relative sound pressure level, in dB, at frequency 200 Hz, for three reception heights (2 m, 5 m and 8 m)

Table A.1 — Insertion loss at a frequency of 100 Hz, for *y* from 0 m to 80 m and *x* from −80 m to 80 m, at a reception height of 8 m

x m	*y* (m): 0	10	20	30	40	50	60	70	80
	Insertion loss dB								
−80	22,8	22,2	20,9	20,0	20,0	21,0	22,9	24,5	24,9
−70	24,7	23,7	21,9	20,9	21,4	23,2	25,2	25,5	24,5
−60	28,0	26,2	23,5	22,7	24,0	26,4	26,5	24,9	23,6
−50	30,5	29,0	26,1	26,2	28,7	28,2	25,6	23,9	23,3
−40	24,3	26,6	31,2	34,9	31,1	26,6	24,6	24,1	24,3
−30	18,7	21,8	28,8	30,5	28,5	26,3	25,8	26,4	27,6
−20	18,8	20,1	23,0	30,9	31,3	30,5	31,7	33,6	35,5
−10	15,0	21,8	28,9	35,3	39,9	49,6	46,5	41,0	38,3
0	10,2	32,1	28,2	31,2	35,3	36,1	35,1	34,1	33,3
10	12,4	25,3	29,6	40,2	44,2	36,9	34,2	32,8	32,0
20	17,8	18,0	25,2	33,5	49,2	41,9	36,4	34,1	32,7
30	16,3	18,8	25,2	34,9	32,1	35,7	39,3	37,3	34,9
40	21,1	24,0	30,1	45,9	30,2	28,5	30,3	33,5	35,6
50	24,4	27,7	46,2	34,9	29,6	26,8	26,4	27,8	30,1
60	23,5	25,2	30,4	30,9	28,1	26,3	25,2	25,3	26,3
70	21,7	22,7	25,5	27,6	26,9	25,7	24,8	24,3	24,5
80	20,5	21,2	23,0	25,1	25,7	25,1	24,4	23,9	23,8

Table A.2 — Insertion loss at a frequency of 100 Hz, for *y* from 0 m to 80 m and *x* from −80 m to 80 m, at a reception height of 5 m

x m	*y* (m): 0	10	20	30	40	50	60	70	80
	Insertion loss dB								
−80	19,8	19,4	18,6	18,1	18,3	19,5	21,4	23,2	23,9
−70	20,6	20,0	19,0	18,5	19,3	21,2	23,3	24,2	23,5
−60	21,7	20,9	19,5	19,4	21,0	23,6	24,6	23,7	22,6
−50	23,8	22,3	20,5	21,2	24,0	25,3	23,9	22,7	22,3
−40	28,3	24,7	22,5	25,1	26,6	24,2	22,9	22,7	23,2
−30	30,7	28,8	28,6	29,5	24,9	23,5	23,8	24,8	26,2
−20	20,5	28,7	32,2	26,8	25,5	26,6	28,6	30,8	32,8
−10	29,8	22,0	38,4	35,0	37,7	39,2	38,1	36,7	35,6
0	8,2	31,7	32,0	36,5	35,0	33,5	32,7	32,1	31,8
10	16,1	26,2	36,5	41,5	34,8	32,5	31,5	30,9	30,6
20	16,3	22,2	35,1	32,8	38,9	36,3	33,6	32,2	31,3
30	23,7	33,9	34,6	27,5	27,6	31,3	34,8	34,7	33,4
40	23,8	27,7	29,3	26,4	24,9	25,5	28,0	31,2	33,6
50	21,2	22,9	25,7	25,3	24,3	23,8	24,5	26,3	28,7

Table A.2 *(continued)*

x m	*y* m								
	0	10	20	30	40	50	60	70	80
	Insertion loss dB								
60	19,7	20,7	23,2	24,2	23,8	23,4	23,3	23,9	25,2
70	18,9	19,6	21,5	23,1	23,4	23,1	22,9	23,0	23,5
80	18,3	18,9	20,4	22,1	22,9	22,9	22,7	22,6	22,8

Table A.3 — Insertion loss at a frequency of 100 Hz, for *y* from 0 m to 80 m and *x* from −80 m to 80 m, at a reception height of 2 m

x m	*y* m								
	0	10	20	30	40	50	60	70	80
	Insertion loss dB								
−80	18,4	18,1	17,5	17,1	17,5	18,7	20,6	22,5	23,3
−70	18,7	18,3	17,6	17,4	18,2	20,2	22,4	23,4	23,0
−60	19,1	18,6	17,7	17,9	19,6	22,3	23,6	23,0	22,2
−50	19,7	18,9	18,0	19,1	22,1	23,8	23,0	22,1	21,8
−40	20,6	19,3	18,8	21,7	24,2	22,9	22,0	22,0	22,6
−30	22,6	20,1	21,3	25,0	22,9	22,2	22,8	24,0	25,5
−20	28,5	22,4	27,0	23,0	23,1	24,9	27,2	29,5	31,6
−10	27,6	37,3	24,9	27,7	31,6	34,1	34,8	34,7	34,2
0	−0,8	36,6	34,1	32,3	31,6	31,3	31,2	31,1	31,0
10	18,1	29,9	37,0	34,2	31,6	30,6	30,2	30,0	29,9
20	25,3	25,0	24,0	27,7	33,7	33,9	32,3	31,3	30,6
30	20,0	22,4	22,9	22,9	25,1	29,3	32,9	33,5	32,6
40	18,6	20,3	22,3	22,3	22,6	24,0	26,8	30,1	32,6
50	17,9	19,1	21,4	22,1	22,1	22,4	23,5	25,5	28,0
60	17,6	18,4	20,5	21,8	22,0	22,0	22,3	23,2	24,7
70	17,4	18,0	19,7	21,3	21,9	22,0	22,0	22,3	23,0
80	17,2	17,7	19,1	20,7	21,7	21,9	21,9	22,0	22,2

Table A.4 — Insertion loss at a frequency 200 Hz, for *y* from 0 m to 80 m and *x* from −80 m to 80 m, at a reception height of 8 m

x m	*y* m								
	0	10	20	30	40	50	60	70	80
	Insertion loss dB								
−80	22,7	24,3	28,8	34,2	35,5	37,7	33,0	28,4	26,8
−70	18,5	20,7	26,9	35,2	39,8	34,3	30,8	28,9	30,2
−60	15,2	17,9	25,8	34,3	28,8	30,7	32,5	34,3	40,2
−50	13,2	16,5	27,6	24,6	25,8	35,5	46,9	43,1	42,7
−40	13,9	17,7	25,4	21,4	29,3	37,1	35,9	38,5	39,5

Table A.4 *(continued)*

x m	*y* m 0	10	20	30	40	50	60	70	80
	Insertion loss dB								
−30	20,1	24,2	21,1	25,2	30,5	31,7	37,1	37,1	35,9
−20	14,9	26,3	36,7	28,3	31,1	37,0	37,9	38,8	37,6
−10	11,2	24,1	45,2	37,7	37,3	35,9	37,6	40,5	41,8
0	12,2	46,9	41,0	35,0	31,1	31,2	32,4	33,9	35,2
10	1,4	20,8	26,0	35,3	28,8	31,3	38,5	49,6	38,3
20	10,2	32,7	31,3	23,5	31,8	34,9	34,0	36,1	43,0
30	13,5	21,2	26,1	20,3	23,4	30,8	60,9	43,2	43,9
40	12,8	14,1	36,1	23,6	23,0	26,3	32,7	49,9	34,9
50	12,0	13,5	23,4	31,8	29,4	27,6	30,6	36,7	51,5
60	14,2	15,4	21,0	39,5	48,4	33,4	29,2	32,6	41,4
70	17,8	18,6	21,9	30,7	37,8	32,3	28,5	27,3	30,2
80	22,7	22,5	23,2	28,0	35,4	30,2	26,9	25,5	25,4

Table A.5 — Insertion loss at a frequency of 200 Hz, for *y* from 0 m to 80 m and *x* from −80 m to 80 m, at a reception height of 5 m

x m	*y* m 0	10	20	30	40	50	60	70	80
	Insertion loss dB								
−80	19,8	20,2	22,8	30,1	26,9	25,7	25,9	24,2	23,4
−70	22,8	23,0	26,7	31,2	27,3	27,8	25,4	24,1	25,7
−60	26,9	27,1	32,8	30,7	31,2	27,6	25,2	27,1	32,5
−50	23,0	27,3	34,8	38,7	31,7	27,1	29,5	37,3	49,2
−40	17,1	23,2	36,9	31,1	31,1	34,4	49,5	44,1	37,0
−30	14,4	23,1	23,8	32,9	46,4	42,2	39,3	35,0	34,5
−20	23,0	26,4	24,8	32,4	36,9	36,0	36,4	38,1	37,9
−10	17,5	27,7	29,3	37,6	38,3	37,0	37,8	38,7	38,8
0	9,6	37,9	35,9	32,1	33,2	35,0	36,3	37,0	37,3
10	9,4	24,5	35,4	31,4	34,7	44,4	34,9	31,2	29,6
20	15,4	25,5	20,6	27,0	47,5	42,3	44,0	54,1	40,9
30	12,9	18,3	26,4	26,2	32,1	43,8	31,7	33,1	38,0
40	15,5	18,3	38,4	35,5	29,0	37,2	42,7	31,5	28,9
50	22,2	22,4	30,1	31,1	26,7	25,9	31,1	37,3	33,0
60	27,0	23,5	25,4	33,4	25,3	23,4	23,8	27,5	32,9
70	22,0	20,8	21,4	31,5	27,1	22,7	21,9	22,6	25,5
80	18,8	18,4	18,8	24,3	33,2	23,7	21,3	21,1	21,9

Table A.6 — Insertion loss at a frequency of 200 Hz, for *y* from 0 m to 80 m and *x* from −80 m to 80 m, at a receiver height of 2 m

x m	*y* m 0	10	20	30	40	50	60	70	80
	Insertion loss dB								
−80	14,0	14,9	18,2	26,4	23,8	22,1	22,8	22,2	21,9
−70	14,6	15,6	20,4	27,4	22,4	23,1	22,6	22,0	23,8
−60	15,4	16,8	24,2	24,4	23,2	23,2	22,2	24,4	29,6
−50	16,7	18,7	29,1	23,5	24,2	22,5	25,4	32,5	40,3
−40	19,1	22,2	26,1	26,1	23,2	27,0	37,0	39,0	34,9
−30	25,6	31,8	28,9	24,6	30,2	41,6	35,7	33,3	33,5
−20	24,6	35,8	29,1	38,2	37,9	33,6	35,1	37,6	38,1
−10	27,9	26,1	38,4	35,5	39,0	37,7	37,3	37,1	37,2
0	−0,8	36,3	36,1	36,6	37,2	37,2	37,0	36,8	36,5
10	26,6	23,4	36,3	39,2	37,1	30,3	27,8	26,8	26,5
20	20,6	33,2	29,0	36,0	28,1	32,5	38,2	38,3	34,3
30	23,4	26,5	23,6	23,4	32,5	29,1	26,9	29,4	33,8
40	17,2	18,5	29,7	20,8	21,7	28,2	30,9	27,6	26,6
50	15,0	15,8	26,2	22,4	19,8	21,0	25,6	30,3	29,2
60	13,9	14,5	19,1	30,9	20,4	19,4	20,6	24,1	28,7
70	13,3	13,7	16,3	28,3	23,6	19,5	19,2	20,3	23,2
80	12,9	13,2	14,9	21,0	32,0	21,1	19,1	19,1	20,2

A.4 Example of use of the benchmark case

In Annex B, the Kirchhoff approximation is described. Formula (B.2) describes the case where a wave travels through one opening. The benchmark case has three openings, which can be calculated separately. First, the wave has to travel through the inner openings, which are formed by the lower end of the baffles. This means that Formula (B.2) has to be applied twice, to describe the sound propagation. The baffles themselves are non-absorbing on both sides, whereas the rest of the inside is absorbing. The reflections are described by introducing mirror sources including the reflection of the openings to describe the propagation correctly. For the model calculation, up to two reflections are assumed. Additionally, the baffles are assumed to be very thin in relation to the wavelength.

The first reflection occurs on the rear of the first baffle, which is at $x = 2$ m and forms the end of the first opening. The model source is then at $x = 7$ m, the lower opening of this source starts at 2 m and goes to 4 m. This source is reflected again at the first baffle at $x = 0$ m, which leads to third mirror source at −7 m and an opening from $x = -4$ m to 2 m. This process is repeated for all three openings. The insertion loss is calculated from the free field of the source positioned at P(−3 m, 0 m, 0 m) and it is assumed that the insertion loss is not more than 30 dB (see ISO 9613-2). This is achieved by adding −30 dB to the negative level of the insertion loss.

The results are depicted in Figure A.4 and Figure A.5, showing on the right side the insertion loss to be compared with the benchmark case and on the left the inclusion of the ground reflection.

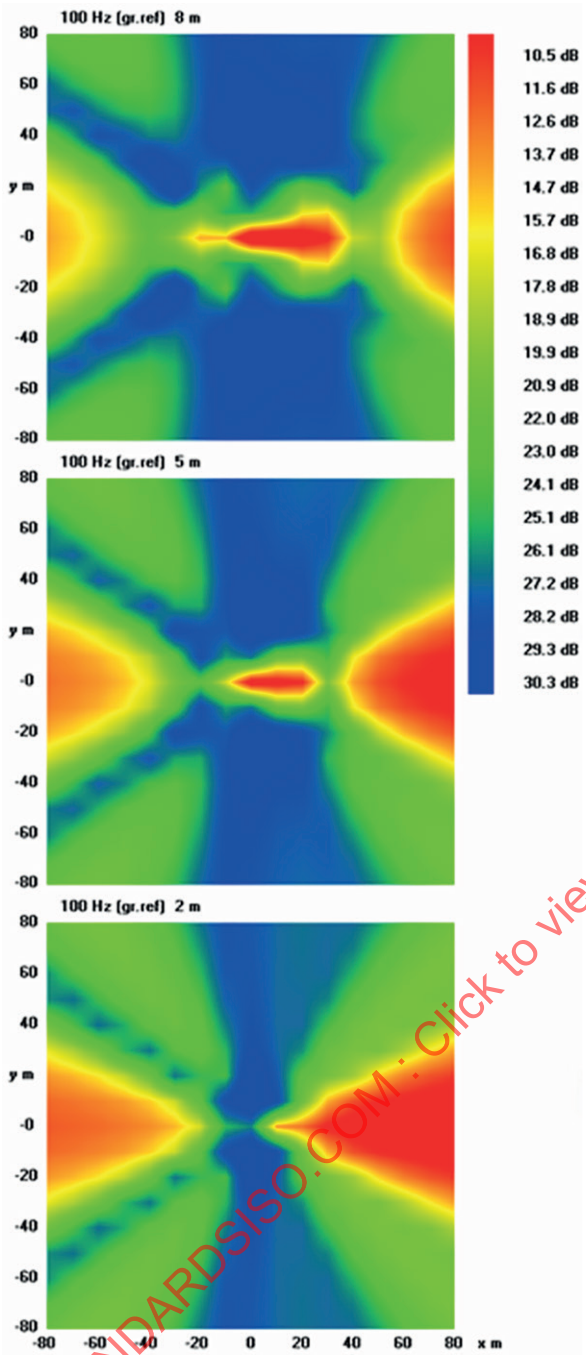

a) Model calculation for 100 Hz

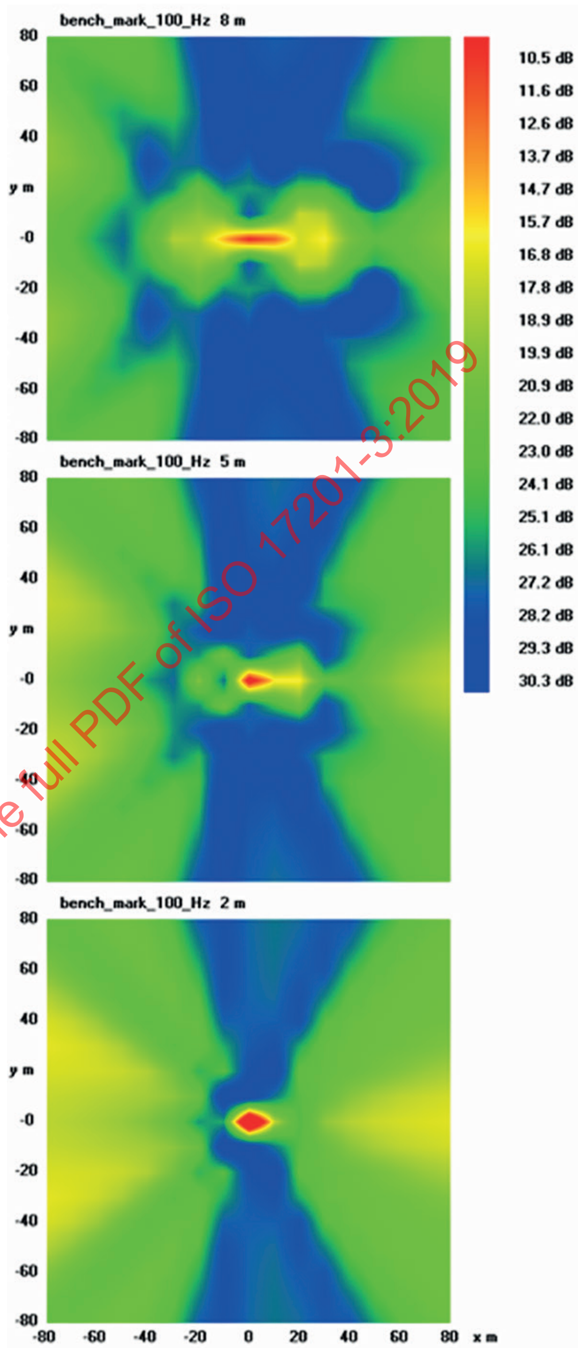

b) Benchmark case for 100 Hz

Figure A.4 — Insertion loss limited to 30 dB (for 100 Hz)

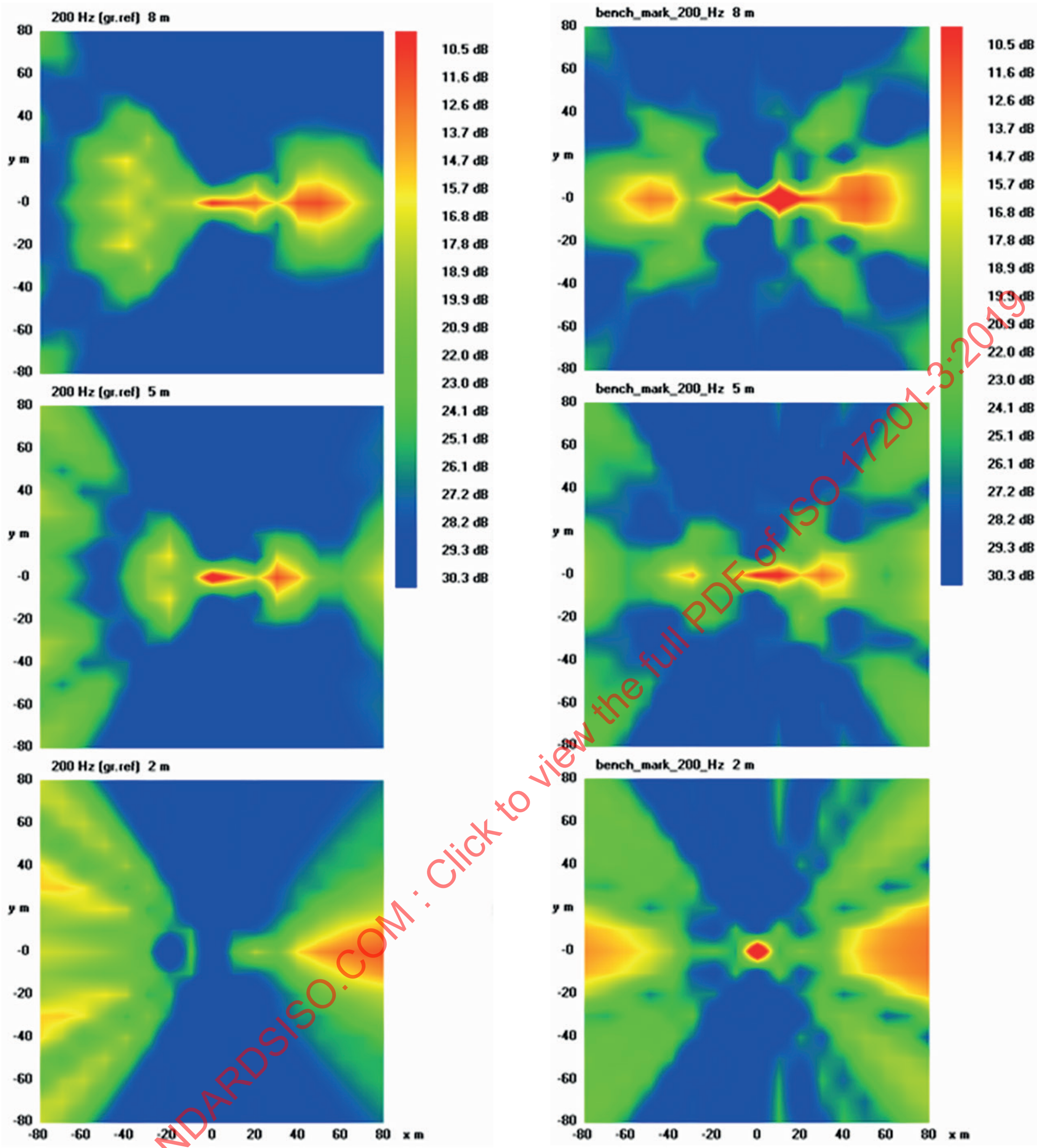

a) Model calculation for 200 Hz

b) Benchmark case for 200 Hz

Figure A.5 — Insertion loss limited to 30 dB (for 200 Hz)

The data for the insertion loss are given in Tables A.7 to A.12.

Table A.7 — Insertion loss for model calculation at a frequency of 100 Hz, with a source P(−3,0 m, 0,0 m, 0,0 m) and a height above ground of 8 m

x m	*y* m								
	0	10	20	30	40	50	60	70	80
	Insertion loss dB								
−80	14,2	14,7	16,3	19,3	24,7	34,0	30,2	25,7	23,7
−70	15,2	15,8	17,9	22,0	30,0	33,2	26,8	24,2	23,1
−60	16,7	17,5	20,3	26,3	36,7	28,6	25,0	23,7	23,2
−50	19,4	20,4	24,3	34,6	31,7	26,4	24,6	24,1	24,3
−40	23,2	25,0	32,0	38,0	29,0	26,2	25,5	25,7	26,5
−30	19,9	25,0	41,4	33,5	29,6	28,2	28,3	29,3	30,6
−20	14,3	23,1	28,7	32,9	33,7	33,5	34,4	35,7	37,2
−10	14,6	26,6	25,7	34,8	44,2	45,4	44,4	43,0	41,7
0	5,6	34,7	38,0	42,5	51,1	46,2	42,0	39,9	38,6
10	5,4	22,7	31,8	40,0	49,2	42,8	39,4	37,8	36,8
20	7,4	16,4	23,2	40,8	46,2	41,4	39,0	37,5	36,5
30	9,9	16,0	25,1	34,5	36,9	36,5	37,1	37,2	36,8
40	18,2	22,1	30,5	30,1	29,2	30,1	31,7	33,5	34,9
50	19,6	20,7	24,8	27,2	25,5	25,7	27,1	29,0	30,8
60	15,1	15,9	19,1	23,7	24,3	23,5	24,1	25,5	27,2
70	12,7	13,4	15,8	19,9	23,2	22,9	22,6	23,3	24,5
80	11,4	11,9	13,8	17,1	21,0	22,6	22,1	22,0	22,7

Table A.8 — Insertion loss model calculation at a frequency of 100 Hz, with a source P(−3,0 m, 0,0 m, 0,0 m) and a height above ground of 5 m

x m	*y* m								
	0	10	20	30	40	50	60	70	80
	Insertion loss dB								
−80	12,6	13,1	14,8	18,0	23,5	32,8	29,0	24,7	22,8
−70	13,0	13,7	15,9	20,2	28,5	31,5	25,5	23,1	22,1
−60	13,7	14,6	17,6	24,0	34,1	26,7	23,5	22,4	22,2
−50	14,8	16,0	20,4	31,1	28,6	24,1	22,8	22,6	23,1
−40	16,7	18,5	25,8	32,5	25,2	23,5	23,4	24,1	25,2
−30	20,8	23,6	38,1	27,5	24,8	24,8	25,8	27,4	29,1
−20	23,8	35,3	33,1	28,1	27,8	29,2	31,3	33,5	35,5
−10	17,3	27,9	34,5	36,0	37,6	39,7	40,7	40,6	39,9
0	8,5	33,9	47,4	50,7	42,6	39,7	38,2	37,4	36,8
10	9,0	22,1	45,6	43,0	38,3	36,6	35,7	35,3	35,0
20	10,1	21,1	34,8	36,2	36,8	36,5	35,8	35,2	34,8
30	21,2	25,9	27,2	26,6	29,4	32,3	34,4	35,2	35,3
40	14,5	16,8	23,2	23,0	23,9	26,5	29,3	31,7	33,5
50	11,6	13,2	18,2	22,2	21,7	22,8	24,9	27,3	29,5

Table A.8 *(continued)*

x m	*y* m								
	0	10	20	30	40	50	60	70	80
	Insertion loss dB								
60	10,3	11,4	15,0	20,2	21,5	21,2	22,3	24,0	26,0
70	9,6	10,4	13,0	17,4	21,0	21,0	21,0	22,0	23,4
80	9,2	9,8	11,8	15,2	19,3	21,1	20,8	20,9	21,8

Table A.9 — Insertion loss for model calculation at a frequency of 100 Hz, with a source P(−3,0 m, 0,0 m, 0,0 m) and a height above ground of 2 m

x m	*y* m								
	0	10	20	30	40	50	60	70	80
	Insertion loss dB								
−80	11,8	12,3	14,0	17,3	22,9	32,3	28,4	24,2	22,4
−70	12,0	12,7	15,0	19,4	27,8	30,6	24,8	22,5	21,7
−60	12,3	13,2	16,4	22,9	32,9	25,7	22,7	21,7	21,6
−50	12,7	14,0	18,7	29,6	27,2	23,0	21,9	21,9	22,5
−40	13,4	15,4	23,1	29,9	23,5	22,1	22,3	23,2	24,5
−30	14,6	18,1	32,3	24,3	22,6	23,2	24,6	26,4	28,3
−20	17,3	24,7	26,1	23,7	24,9	27,3	29,9	32,4	34,7
−10	26,7	33,6	26,9	29,6	33,7	37,2	39,1	39,4	39,1
0	29,8	41,5	46,6	40,2	38,1	37,1	36,5	36,2	35,9
10	14,3	33,1	35,1	34,6	34,2	34,1	34,1	34,1	34,2
20	13,0	21,4	23,4	30,0	33,7	34,5	34,4	34,2	34,0
30	9,7	14,8	20,1	22,0	26,6	30,6	33,1	34,3	34,6
40	8,8	11,6	18,9	19,9	21,6	24,8	28,1	30,8	32,8
50	8,5	10,1	15,6	20,0	20,0	21,4	23,9	26,5	28,9
60	8,3	9,4	13,2	18,6	20,1	20,1	21,3	23,3	25,4
70	8,2	9,0	11,7	16,2	19,9	20,1	20,2	21,3	22,9
80	8,1	8,7	10,8	14,3	18,5	20,3	20,1	20,3	21,3

Table A.10 — Insertion loss for model calculation at a frequency of 200 Hz, with a source P(−3,0 m, 0,0 m, 0,0 m) and a height above ground of 8 m

x m	*y* m								
	0	10	20	30	40	50	60	70	80
	Insertion loss dB								
−80	34,4	36,7	34,8	29,5	28,1	33,0	32,1	25,7	24,2
−70	28,3	31,3	31,3	32,3	36,9	40,7	30,0	27,0	27,6
−60	22,6	26,0	23,9	27,0	38,3	35,1	32,4	32,1	34,6
−50	18,8	22,3	18,6	25,4	28,9	31,0	38,2	42,0	43,3
−40	17,0	19,0	16,3	25,4	23,1	30,4	40,4	47,8	49,5

Table A.10 *(continued)*

x m	*y* m 0	10	20	30	40	50	60	70	80
	Insertion loss dB								
−30	20,7	17,8	21,7	19,0	25,4	35,5	45,2	49,2	46,6
−20	18,8	22,6	23,1	26,2	36,2	38,6	40,8	47,2	50,0
−10	18,1	22,6	30,8	38,8	35,1	41,5	51,4	57,3	58,2
0	10,6	34,4	42,7	52,1	46,1	47,1	50,3	54,2	58,7
10	12,5	30,2	36,8	35,0	32,6	35,7	41,2	50,2	61,3
20	13,0	19,4	43,6	39,1	34,3	38,5	43,0	49,8	51,3
30	16,1	31,1	26,6	31,6	41,1	39,9	42,3	48,6	48,7
40	12,1	16,9	22,4	25,9	35,8	46,5	50,6	49,0	44,9
50	11,6	16,2	20,0	26,8	32,2	44,8	60,5	56,2	47,3
60	14,1	18,0	22,1	27,1	34,0	44,0	52,4	47,3	48,4
70	18,1	21,3	26,6	29,4	36,1	43,5	43,5	41,9	42,4
80	23,0	25,8	32,8	35,6	38,6	38,9	37,3	37,3	38,3

Table A.11 — Insertion loss for model calculation at a frequency of 200 Hz, with a source P(−3,0 m, 0,0 m, 0,0 m) and a height above ground of 5 m

x m	*y* m 0	10	20	30	40	50	60	70	80
	Insertion loss dB								
−80	21,9	24,1	23,0	18,9	19,1	25,2	25,6	20,6	19,9
−70	24,2	26,8	23,4	19,9	23,0	29,1	22,0	20,7	22,5
−60	28,6	31,4	24,7	22,9	31,2	24,5	22,0	23,9	28,1
−50	35,8	37,4	29,4	31,2	29,6	24,4	26,2	31,0	35,3
−40	25,4	28,2	32,4	39,7	29,9	30,8	35,5	39,0	41,0
−30	19,5	19,4	28,1	29,7	40,6	42,7	44,7	40,7	37,1
−20	20,6	16,5	20,5	30,2	44,6	48,8	41,7	39,7	40,0
−10	21,6	24,9	30,4	38,2	43,5	52,1	51,9	53,3	52,8
0	6,2	36,7	51,0	44,9	49,0	56,0	65,3	69,8	66,5
10	12,9	31,2	37,0	35,6	42,6	55,3	44,9	42,2	41,2
20	17,0	32,9	31,9	41,1	43,9	48,1	43,1	39,6	37,6
30	11,8	17,4	26,0	41,9	64,1	46,0	40,2	39,0	38,7
40	15,0	21,2	27,9	40,1	47,7	46,5	45,5	38,6	36,2
50	21,9	28,6	34,0	39,5	37,9	38,9	41,3	44,3	39,9
60	24,6	28,3	34,3	35,9	33,0	33,3	36,0	38,7	41,9
70	20,1	22,5	26,9	29,5	31,4	30,2	31,6	34,5	37,1
80	17,3	19,3	23,3	25,7	28,6	29,3	29,0	30,9	33,6

Table A.12 — Insertion loss for model calculation at a frequency of 200 Hz, with a source P(−3,0 m, 0,0 m, 0,0 m) and a height above ground of 2 m

x m	*y* m 0	10	20	30	40	50	60	70	80
	Insertion loss dB								
−80	17,6	19,9	19,1	15,4	16,1	22,5	23,0	18,5	18,1
−70	18,0	20,8	18,1	15,4	19,1	25,4	19,1	18,2	20,4
−60	18,7	21,8	17,1	16,7	25,5	20,1	18,5	21,0	25,6
−50	19,6	22,5	16,6	21,3	22,1	18,9	21,8	27,4	32,3
−40	21,4	22,3	18,3	26,0	19,6	23,2	29,6	34,6	37,7
−30	25,5	22,1	27,4	21,1	25,5	32,5	37,9	36,0	33,6
−20	46,9	29,1	25,8	30,0	37,5	37,1	34,2	34,6	36,3
−10	25,0	27,3	40,6	41,5	37,4	40,2	44,8	48,5	48,8
0	41,0	41,6	58,7	57,9	53,2	53,0	53,8	55,0	56,3
10	25,8	31,8	45,7	38,2	35,5	35,3	35,8	36,5	37,2
20	18,6	31,2	40,2	41,9	35,6	36,2	35,5	34,4	33,9
30	21,9	27,9	29,7	35,0	42,3	36,1	33,6	34,3	35,2
40	16,1	21,2	27,3	27,6	33,4	38,8	39,7	34,5	33,0
50	14,0	18,3	22,5	26,6	27,6	32,7	37,0	40,7	37,1
60	13,0	16,4	20,4	24,8	26,0	27,9	32,2	35,9	39,4
70	12,5	15,0	19,3	22,0	25,8	25,9	28,2	31,9	35,1
80	12,1	14,1	18,3	20,5	24,0	25,8	26,1	28,5	31,7

Table A.13 provides the results gathered by comparing the model calculation with the benchmark case.

Table A.13 — Comparison of the model calculation to benchmark case

Frequency *f* Hz	**Height** *h* m	**Difference** dB	**Standard deviation** dB	**Average level** dB	**Correlation coefficient** 1
100	8	−1,3	3,5	76,6	0,67
100	5	−1,0	3,5	79,2	0,67
100	2	−0,9	3,5	80,6	0,79
200	8	1,1	2,3	76,9	0,77
200	5	0,6	3,2	75,7	0,58
200	2	0,7	3,9	81,3	0,71

The difference is negative if the model leads to higher levels compared to the benchmark for all points where the absolute value of *x* or *y* is greater than or equal to 60 m. For 100 Hz, the model overestimates on the average by 1,1 dB and underestimates by 0,8 dB at 200 Hz. The average standard deviation is 3,5 dB at 100 Hz and 3,1 dB at 200 Hz. The correlation coefficient is between 0,5 and 0,8. These values are obtained by adding a level of −30 dB to the negative insertion losses of the model and the benchmark case.

If 2 dB are added to the above result for the model calculation, underestimations can be ruled out and the overestimation may reach 6 dB in extreme cases. The comparison is not of the sound energy travelling in the different directions but that of the sound exposure levels, which includes ground reflections producing additional interference, with a tendency to lead to large deviations if the phase shifts are different in the benchmark case compared to the model.

The latter can be seen from Figure A.6, which depicts only the insertion loss without ground reflection; interference does not occur and the spatial structure is far simpler:

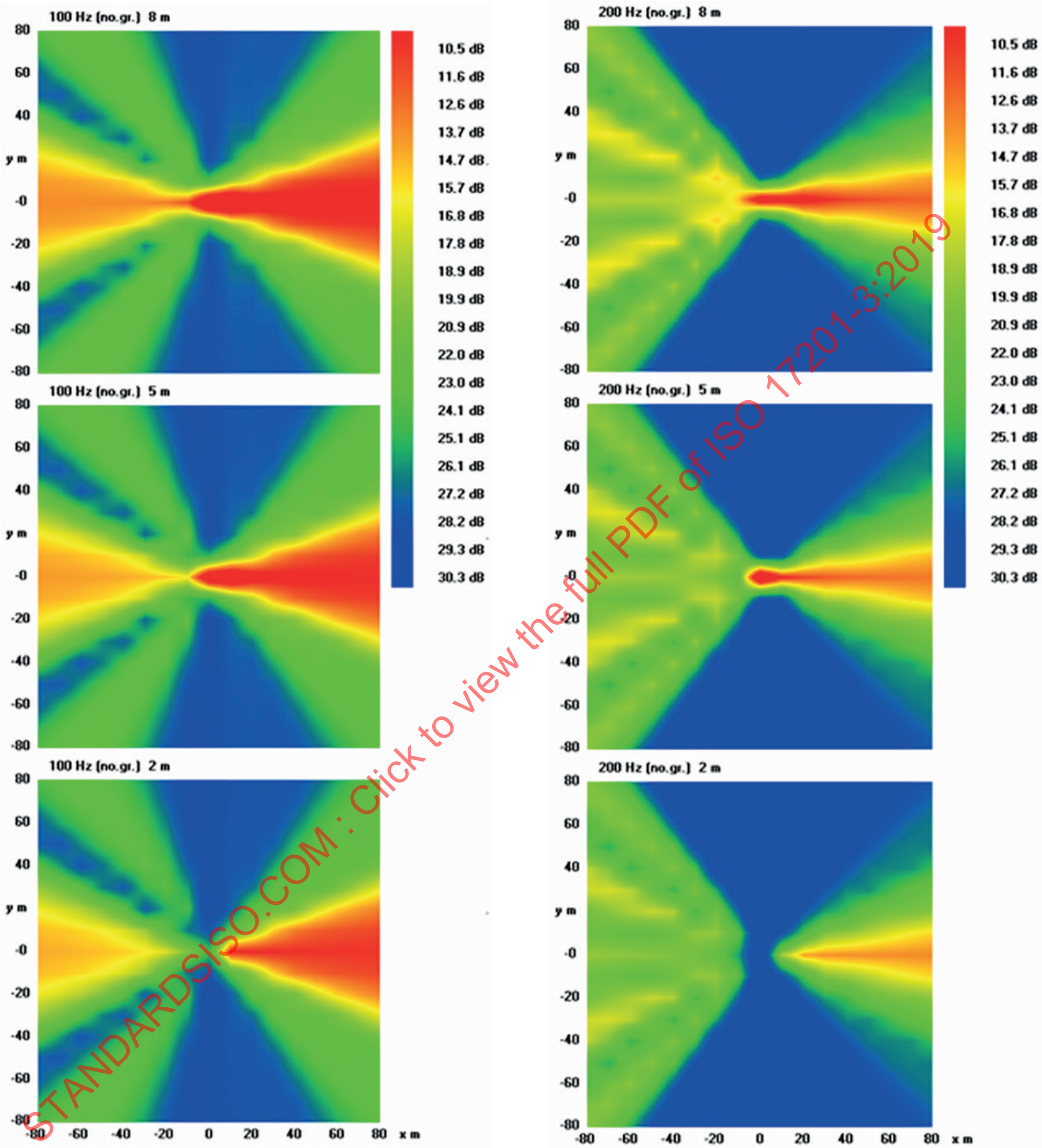

a) Insertion loss of the direct wave for 100 Hz without ground reflection

b) Insertion loss of the direct wave for 200 Hz without ground reflection

Figure A.6 — Insertion loss for three heights

The energy flow is very close to what is observed from the benchmark case [see Figure A.4 b) and Figure A.5 b)] for the distribution of sound energy into the different horizontal directions. For larger distances, the case for a height of 5 m can be considered to be the most representative for the radiation of sound energy into the surrounding. If the sound exposure levels are calculated for greater distances without ground reflection, these levels can be used directly to calculate both the angular source energy distribution levels and the directivity as described in ISO 17201-1. The propagation calculation for the substitute source is described in Annex C. For the benchmark case, the substitute source should be positioned in the first opening at P(1,0,4).

Using the model specified above, the sound exposure levels for a distance at 500 m as given in Table A.14 are obtained:

Table A.14 — Free-field sound exposure levels at a distance of 500 m

Centre frequency one third octave band f Hz	Angle °[a]												
	0	15	30	45	60	75	90	105	120	135	150	165	180
	Sound exposure level L_E[b] dB												
31,5	65,8	65,6	65,0	64,0	62,6	60,9	59,1	57,2	55,2	53,7	53,2	53,6	53,8
40	68,7	68,4	67,4	65,7	63,4	60,6	57,5	54,3	52,5	54,4	57,1	58,8	59,4
50	69,9	69,4	68,0	65,4	61,6	56,8	51,3	48,8	53,3	57,4	59,9	61,2	61,5
63	71,4	70,7	68,3	63,8	56,4	45,9	41,0	45,8	51,4	55,3	58,3	61,5	62,8
80	71,0	69,9	65,8	56,2	46,8	48,2	49,1	49,1	44,5	53,3	64,5	70,2	72,0
100	69,1	67,1	58,3	53,6	54,6	50,8	52,7	50,7	57,4	55,1	63,2	70,9	72,7
125	71,9	67,8	56,1	58,2	48,2	45,2	40,6	51,7	60,2	60,4	47,9	56,9	63,2
160	76,1	69,8	66,9	57,8	49,8	48,5	52,3	54,7	42,8	53,5	60,3	64,0	71,2
200	69,0	62,4	64,9	54,2	48,4	44,6	46,2	30,8	49,1	58,7	68,4	63,9	72,0
250	72,0	65,7	52,8	24,2	38,9	39,2	35,2	38,3	60,7	46,1	56,3	67,1	72,6
315	68,1	63,0	62,6	51,5	49,6	39,3	34,0	42,4	56,2	59,8	60,5	63,1	70,4
400	71,9	65,9	61,9	54,3	51,9	45,4	42,8	44,9	48,8	57,2	63,2	54,6	68,8
500	74,4	71,7	60,0	44,3	49,2	41,1	27,6	34,1	46,8	51,3	57,5	63,5	69,7
630	68,4	68,7	62,7	39,1	43,6	37,5	31,0	37,1	33,6	57,4	54,2	60,7	62,6
800	62,5	60,1	62,4	54,4	44,4	39,2	35,3	31,2	42,6	44,3	52,6	61,9	57,2
1 000	58,8	64,0	65,6	46,0	42,6	24,1	29,7	32,1	38,5	45,5	41,6	60,0	62,2

[a] There are 13 directions based on an angular source energy distribution level of 140 dB within the benchmark shed at 8 m above ground at a distance of 500 m. The 2 dB addition and the 30 dB maximum insertion loss are not incorporated in values given.

[b] The sound exposure level to be used in Formula (3) to calculate $L_{q,S}$ (α,f).

Annex B
(informative)

Sophisticated modelling approaches

B.1 Preliminary remarks

A very sophisticated way of solving the wave-equation is BEM. This has been used for the benchmark case and is briefly described in Annex A.

Another approach to solve the wave equation is represented by the Kirchhoff integral solution.

Ray tracing is done under the assumption that the wavelength is very small in relation to changes in the speed of sound. However, this method can be improved by assuming that the diameter of the ray depends on the wavelength and the distance between source and reception point. The diameter is assumed to be a half of the first Fresnel zone, the diffraction can then be described using the Kirchhoff integral formulation or the approximations described in Reference [23] or the Maekawa approximation (Reference [11]).

B.2 Kirchhoff approximation

The Kirchhoff integral formulation[27] assumes that pressure field is known over the closed surface to calculate the field within the enclosed volume. In the following, the simple case is described where the line of fire is parallel to the x-direction and the shed is completely absorbing on the inside with the exception of the ground and has a rectangular opening at $x = 0$ in the y z-plane. The shooting shed has a length in $-x$ direction, l, which is larger than the distance from the muzzle position to its opening through which the shots are fired. The approximation is to assume that the sound pressure is zero on the outside surface of the shed including the rear.

The height of the shed is l_Z and its width l_Y. The surface of the shed (inside) is assumed to be absorbing, so that the reflection especially from the inside of the roof can be neglected. The floor of the shed is assumed to be acoustically hard with infinite impedance and a reflection coefficient of 1, where h_{ground} is the height of the floor above ground.

The sound exposure level, $L_E(x, y, z, f)$, of the muzzle blast as seen from reception point P(x, y, z) can be written as:

$$L_E(x,y,z,f)=10\lg\left[\left(\frac{2\pi}{\lambda}\right)^2\frac{q_{k_0}^2 F_0}{S_0}\right]\text{dB} \tag{B.1}$$

where

$$\begin{aligned} q_{k_0} = & \int_F \frac{\sqrt{S(\beta)}\,\mathrm{e}^{\mathrm{i}\left[k_0(r_0+r_1)\right]}\left[(1/\mathrm{i}k_0 r_0+1)\cos\beta+(1/\mathrm{i}k_0 r_1+1)\cos\alpha\right]}{4\pi r_0 r_1}\,\mathrm{d}y'\mathrm{d}z' + \\ & Q(f)\int_F \frac{\sqrt{S(\beta')}\,\mathrm{e}^{\mathrm{i}\left[k_0(r_0'+r_1)\right]}\left[(1/\mathrm{i}k_0 r_0'+1)\cos\beta'+(1/\mathrm{i}k_0 r_1+1)\cos\alpha\right]}{4\pi r_0' r_1}\,\mathrm{d}y'\mathrm{d}z' \end{aligned} \tag{B.2}$$

where

r_0 is the distance, in metres, of the vector pointing from the muzzle position P(x_0, y_0, z_0) to point P(0, y', z') in the open surface of the shed, denoted by y', z';

r'_0 is the distance, in metres, of the vector pointing from the mirror source position P(x_0, y_0, $-z_0$) to point P(0, y', z') in the open surface of the shed denoted by y', z';

r_1 is the distance, in metres, of the vector from the position P(0, y', z') to the reception point P(x, y, z);

k_0 is the magnitude of the wave vector (2π/λ) of the direct and reflected wave;

λ is the wave length, in metres;

α is the angle, in radians, between the vector r_1 and the normal vector of the opening (shooting direction);

β ,β' are the angles, in radians, between the vector r_0 and the vector r'_0, respectively, and normal vector of the opening (shooting direction);

$Q(f)$ is the reflection factor; see Reference [24];

$S(\beta)$ is the angular source energy distribution, expressed in joules per steradian, of the weapon ammunition combination fired within the shed, as measured according to ISO 17201-1 or calculated using ISO 17201-2: the shooting direction is perpendicular to the plane of the shed opening;

F is the opening area, in square metres;

F_0 is 1 m^2.

NOTE 1 The integration is done over the area, F, of the opening. S_0 is the reference angular source energy distribution, S_0 = 10^{-12}Jsr^{-1}.

Figure B.1 illustrates the situation.

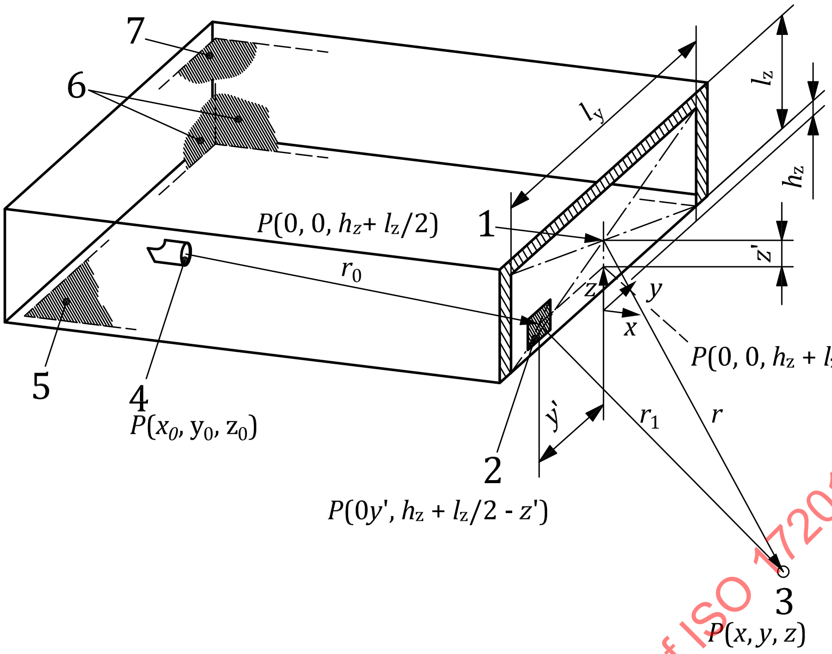

Key

1 middle of opening
2 element ΔF
3 reception point
4 muzzle
5 ground (reflecting)
6 absorbing surface elements of wall
7 absorbing surface elements of roof

Figure B.1 — Description of the model situation

The angular source energy distribution level of the substitute source (see Annex C) is obtained from:

$$L_q(\alpha, f) = 10\lg\left[\left(\frac{2\pi}{\lambda}\right)^2 \frac{q_{k_0}^2 F_0}{S_0}\right] - 11\,\mathrm{dB} + 10\lg\left(\frac{r^2}{F_0}\right)\mathrm{dB} \tag{B.3}$$

where

α is the angle between the line from the middle of the shed opening to the reception point P(x, y, z) to the normal of the opening;

F_0 is 1 m^2.

The shooting direction is perpendicular to the plane of the shed opening. The impedance of the ground is assumed to be infinite. Reflection factor, $Q(f)$, is assumed to be 1 due to the observation that the angle of incidence is close to normal incidence.

Formula (B.3) is based on the assumption that the square root of the angular source energy distribution produced by the muzzle blast in the shed opening produces an elementary source, which can be described as a breathing sphere having a surface of dy'·dz'/2π which radiates into the open space. For numerical integration, dy' should be equal to dz' and these quantities shall be small compared to the wavelength, so that 1>> k_0dz'. For details, see for example Reference [25].

An example for a substitute angular source energy distribution level, $L_{q,\mathrm{S}}$, and its frequency dependence is shown in Figure B.2 for a 15 m deep shed with a height of 2,5 m and a width of 12 m. The bottom of the shed is not elevated from the ground (h_{ground} = 0). The gun has an angular source energy distribution level of 140 dB in each frequency band and no directivity (see Figure B.2). The gun is positioned in the middle of the shed 12 m from the opening 1,5 m above the bottom of the shed. The angular source energy distribution level, $L_{q,\mathrm{S}}$, of the substitute source has been calculated for a point P (1 000 m, 0 m, 1,3 m) in the shooting direction. Calculation results performed for point P (1 000 m, 0 m, 1,3 m) are shown in Figure B.2.

Line b represents the angular source energy distribution level at 1 m distance under free-field conditions. Line a represents the angular source energy distribution level of the substitute source positioned in the middle of the shed opening. Line c shows the difference between the two angular source energy distribution levels.

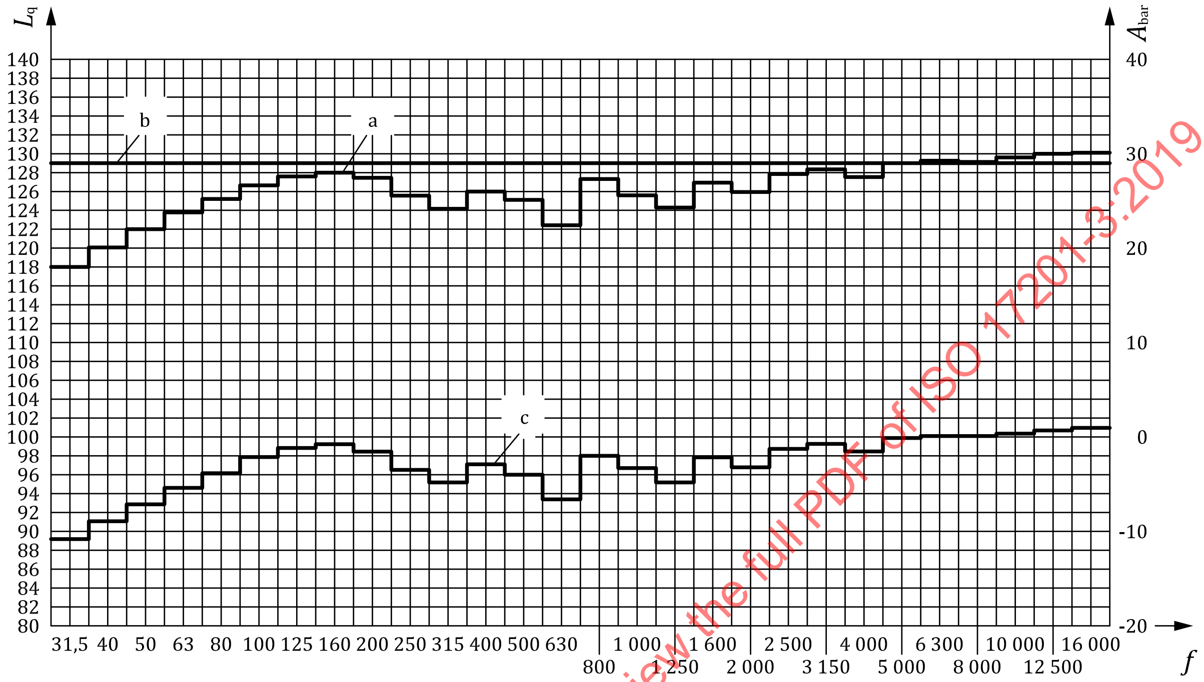

Key

A_{bar} insertion loss, in decibels

f frequency, in hertz

L_q angular source energy distribution level, in decibels

a angular source energy distribution level, in decibels, of the substitute source according to Formula (B.3)

b angular source energy distribution level, in decibels, under free-field conditions

c difference between the two angular source energy distribution levels, in decibels

NOTE The angular source energy distribution level of the muzzle blast under free-field condition is assumed to have no directivity.

Figure B.2 — Angular source energy distribution level for points in the shooting direction for a uniform source energy of 140 dB fired with a muzzle 12 m inside the shed in the middle, 1,5 m above ground, substitute source, reception point P(1 000 m, 0 m, 1,3 m), ground reflection (hard)

The angular source energy distribution level at 315 Hz is 5 dB below the free-field level. This is caused by interference. The reduction for lower frequencies (less than 100 Hz) will only be achieved if the absorption in this frequency range inside the shed is at least more than 90 % for the walls and the ceiling within the shed. The reflections may be accounted for by adding additional reflection sources or by limiting the level reduction proportional to the absorption to be expected.

The same calculation as performed for Figure B.2 has been done for $L_{q,S}$ representing the substitute source for a point at 1 000 m perpendicular to the line of fire. The results are shown in Figure B.3.

Key

A_{bar}	insertion loss, in decibels
f	frequency, in hertz
L_q	angular source energy distribution level, in decibels
a	Angular source energy distribution level, in decibels, of the substitute source according to Formula (B.3).
b	Angular source energy distribution level, in decibels, under free-field conditions.
c	Difference between the two angular source energy distribution levels, in decibels.

NOTE 1 The angular source energy distribution level of the muzzle blast under free-field condition is assumed to have no directivity.

NOTE 2 See Figure B.2.

Figure B.3 — Angular source energy distribution level for 90° to the line of fire at 1 000 m distance, substitute source, reception point P(0 m, 1 000 m, 1,3 m), ground reflection (hard)

Clearly, a considerable reduction is observed. However, due to scattering, the reduction has been limited to values of 30 dB.

In Figure B.4, the substitute angular source energy distribution level, $L_{q,S}$(100 m, 100 m, 4 m), with the gun positioned 6 m from the opening at the centre is depicted.

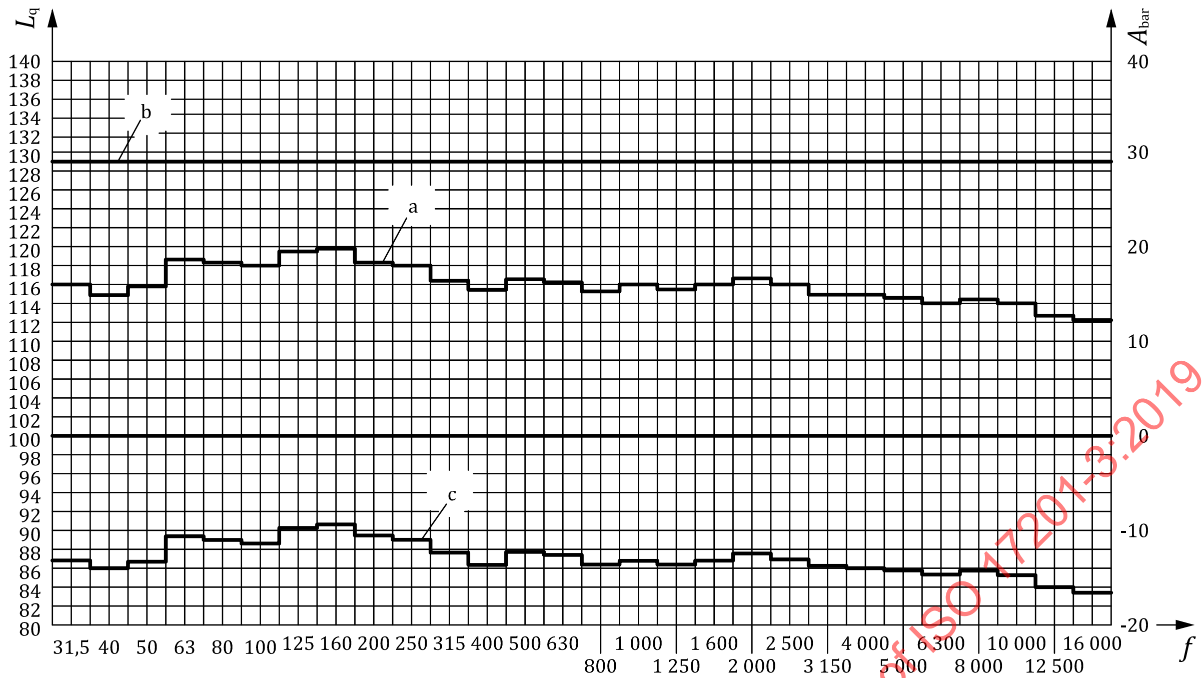

Key

A_{bar} insertion loss, in decibels

f frequency, in hertz

L_q angular source energy distribution level, in decibels

a Angular source energy distribution level, in decibels, of the substitute source according to Formula (B.3).

b Angular source energy distribution level, in decibels, under free-field conditions.

c Difference between the two angular source energy distribution levels, in decibels.

NOTE The angular source energy distribution level of the muzzle blast under free-field condition is assumed to have no directivity.

Figure B.4 — Angular source energy distribution level for gun position in the middle, 6 m from the shed opening, under 45° to the line of fire, substitute source, reception point P(100 m, 100 m, 4 m), ground reflection (hard), ground reflection inside the shed

Figure B.5 shows the same situation as Figure B.6 for a gun, position 4 m off the middle, 12 m from the opening.

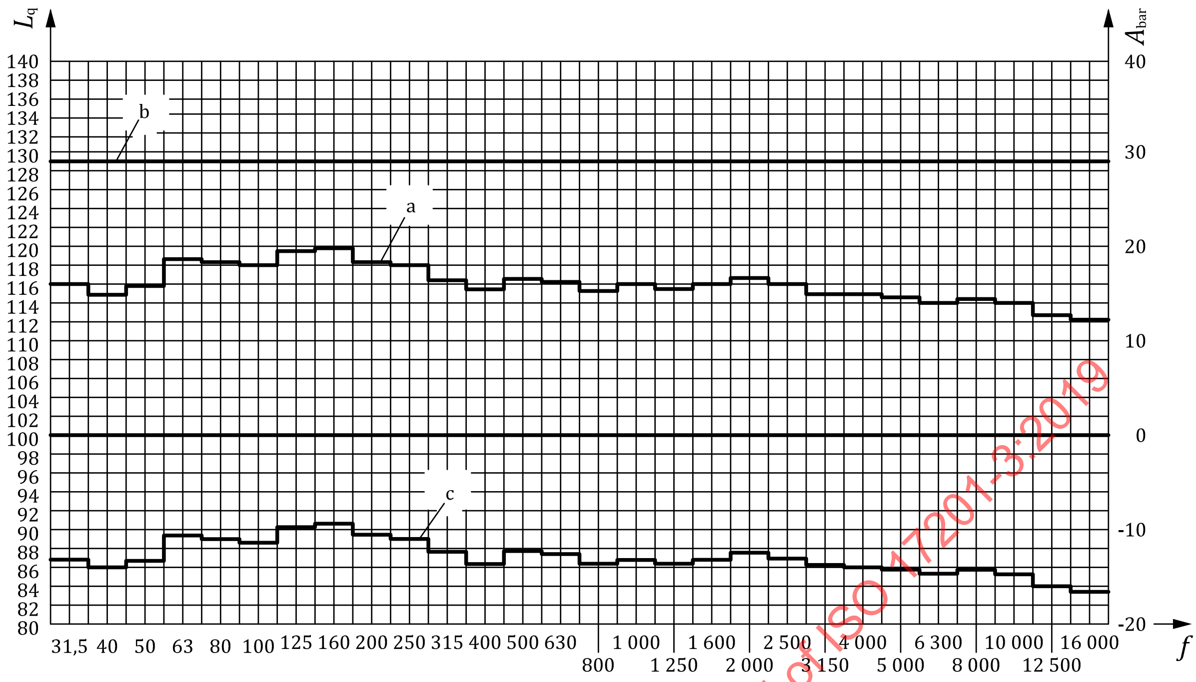

Key

A_{bar}	insertion loss, in decibels
f	frequency, in hertz
L_q	angular source energy distribution level, in decibels
a	Angular source energy distribution level, in decibels, of the substitute source according to Formula (B.3).
b	Angular source energy distribution level, in decibels, under free-field conditions.
c	Difference between the two angular source energy distribution levels, in decibels.

NOTE The angular source energy distribution level of the muzzle blast under free-field condition is assumed to have no directivity.

Figure B.5 — Angular source energy distribution level for 45° to the line of fire and its substitute source, for the muzzle at 6 m from the opening and 2 metres off-centre in the direction of reception point P(100 m, 100 m, 4 m), ground reflection (hard)

Figure B.6 shows the same situation: muzzle position plus 2 m off-centre in the middle, 6 m from the opening using the angular source energy distribution level as given in Table C.3, for a reception point position P(100 m, 100 m, 4 m).

The differences of the insertion loss are caused by the directivity.

NOTE 2 The insertion loss has been limited to 30 dB as in Annex A.

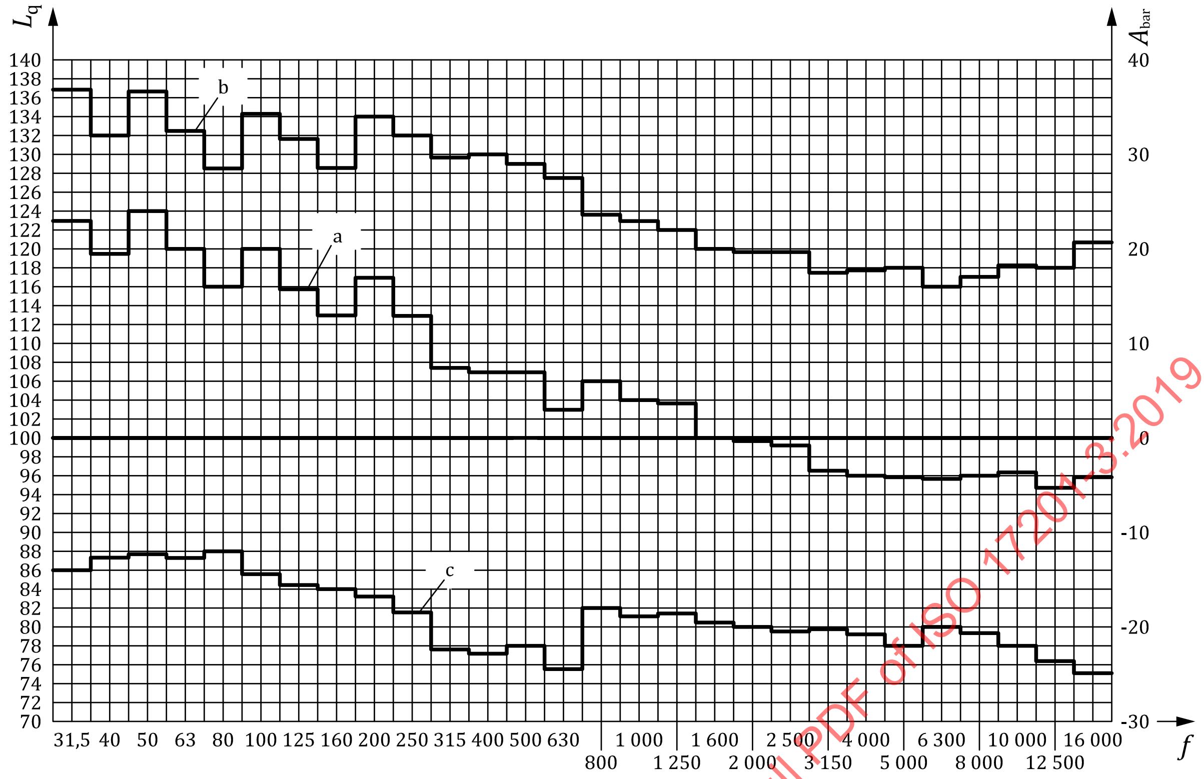

Key

A_{bar} insertion loss, in decibels

f frequency, in hertz

L_q angular source energy distribution level, in decibels

a Angular source energy distribution level, in decibels, of the substitute source according to Formula (B.3).

b Angular source energy distribution level, in decibels, under free-field conditions.

c Difference between the two angular source energy distribution levels, in decibels.

NOTE Directivity of a full choke, 0,7 m barrel length, muzzle speed 400 m/s.

Figure B.6 — Angular source energy distribution level according to Table C.3 and its substitute source, for the muzzle 6 m from the opening and 2 metres off-centre in the direction of reception point P(100 m, 100 m, 4 m), ground reflection (hard), directivity causes insertion loss differences

B.3 Ray-tracing models

Ray-tracing models assume that the wavelength of the sound wave is small in relation to the size of bodies, which the wave may encounter, when travelling from the source to the reception point. The wave path is governed by the principle formulated by Fermat, which specifies that the ray takes the path which leads to the smallest time span for the wave to travel from source to the reception point. The latter is especially important, when the wave travels through a moving atmosphere, with different local temperatures and wind vectors. If the ray hits an obstacle, the ray is reflected and if this occurs at the edge of an obstacle, diffraction is assumed and its effect has to be approximated. Ray-tracing models can be differentiated according to the approximation they incorporate.

For the purpose of calculating the sound exposure levels resulting from a shot fired in a shed, a non-refracting atmosphere is sufficient. However, diffraction can be described as occurring either at a barrier of finite thickness or at a wedge as described in Reference [23] for example. Either of these solutions may be used. Another alternative is the far simpler Maekawa approximation (Reference [11]), which is described, in brief, in B.4.

B.4 Maekawa approximation

The shooting shed has a length l from the muzzle position to its opening through which the shots are fired. The height of the shed is l_Z and its width l_Y. The surface of the shed (inside) is assumed to be absorbing, so that reflections from the inside of the roof can be neglected. The floor of the shed is assumed to be acoustically hard with infinite impedance and a reflection coefficient of 1.

The substitute source is positioned at the point with the co-ordinates P(0 m, 0 m, 0 m) in the centre of the opening. The sound exposure level, $L_E(x, y, z, f)$, at reception point P(x, y, z) can be calculated using the following steps:

1) Find the diffraction point on the edge of the opening of the shed (this diffraction point corresponds to the shortest diffraction path from source to reception point).

2) Calculate the barrier attenuation according to Maekawa's formula $D = 10 \lg (20\ N + 3)$ dB (see ISO 9613-2 and Reference [11]), with Fresnel number $N = 2\ \delta/\lambda$, where δ is the path length difference, and λ is the wavelength. Use a lower limit of 0,1 for N, so $D \geq 0$ (negative values of N and δ correspond to source-reception point lines "above" the line of sight).

3) The source strength of the substitute source for a specific reception point is equal to the source strength in the direction of the diffraction point diminished by the calculated barrier attenuation from step 2). The substitute source is located in the middle of the opening of the shed with the same height as the original source.

The other damping terms are calculated as if the original source with the surrounding shed was replaced by the substitute source alone. In this simulation model, the acoustical characteristics of the floor at the location of the modelled shed shall be the same as the characteristics of the surrounding ground.

Annex C
(informative)

Modelling of shooting scenarios — Examples of shooting ranges

C.1 Preliminary remarks

This annex shows some practical situations in shooting ranges as examples which can be used to model a shooting range using available software. Calculations of the sound exposure level at reception point are given. In Clauses C.2 and C.3, free-field shooting ranges are given, while Clause C.4 deals with shooting sheds. In Clause C.5, more complex situations are depicted, for which sound exposure levels can be calculated as shown in Clauses B.1 and B.2.

C.2 Free-field ranges

C.2.1 General overview

A general overview of a free-field range is given in Figure C.1 for the most general case of free-field rifle shooting. Figure C.2 shows the case of a skeet range with a typical shooting direction and the resulting unsafe area.

Dimensions in metres

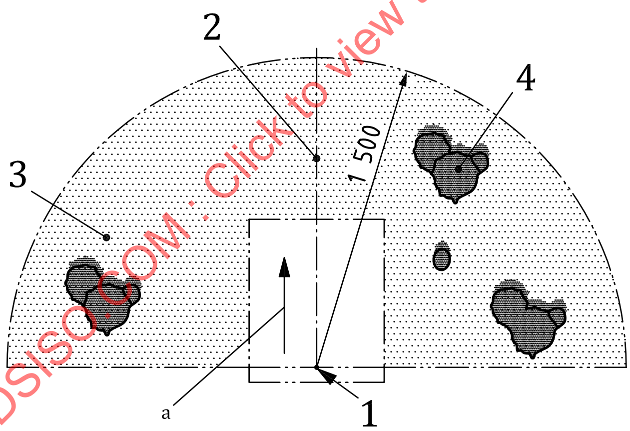

Key

1 firing zone
2 target line
3 unsafe area
4 plants (bushes, trees)
a Firing direction.

Figure C.1 — Free-field situation (most general case) adapted from Reference [26]

Dimensions in metres

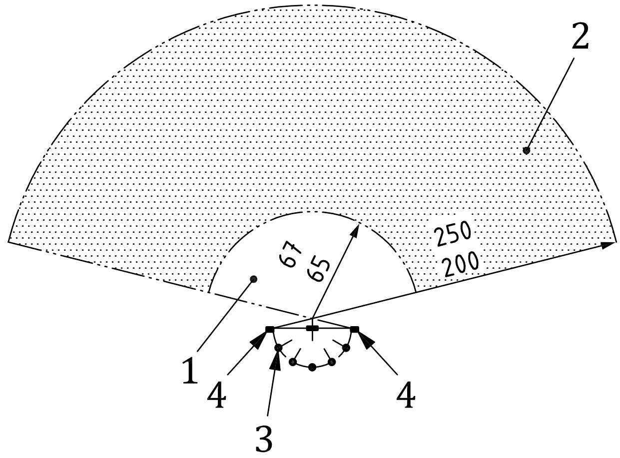

Key

1 clay target falling zone

2 unsafe area

3 firing position

4 launchers

Figure C.2 — Free-field situation (skeet case); adapted from Reference [26]

Firing angles for skeet ranges can vary from −90° to +90° in the horizontal plane and from −10° to +80° in the vertical plane. For trap ranges, the direction falls within −60° to +60° to direction of the range and from 10° to 45° for the vertical direction. The different shooting directions and the different positions of the shooter have to be accounted for.

For certain disciplines, one or more shooter(s) can shoot sequentially or randomly from different positions in the stand. Typical situations are skeet, trap or practical shooting (or speed sport shooting).

NOTE 1 For some disciplines, the target is moving. For instance, clay targets fly from their launchers, or running targets move on a horizontal line (e.g. "rabbit"). For other ones, the shooter is moving (e. g. speed sport shooting).

NOTE 2 Examples of these kinds of situations can be found in books edited by shooting federations (see Reference [26]).

Figure C.3 gives an example for Olympic trap shooting. In this case, five shooters placed on a line fire sequentially in the same stand.

Figure C.4 gives an example for skeet shooting. In this case, there are seven shooters on a circular arc.

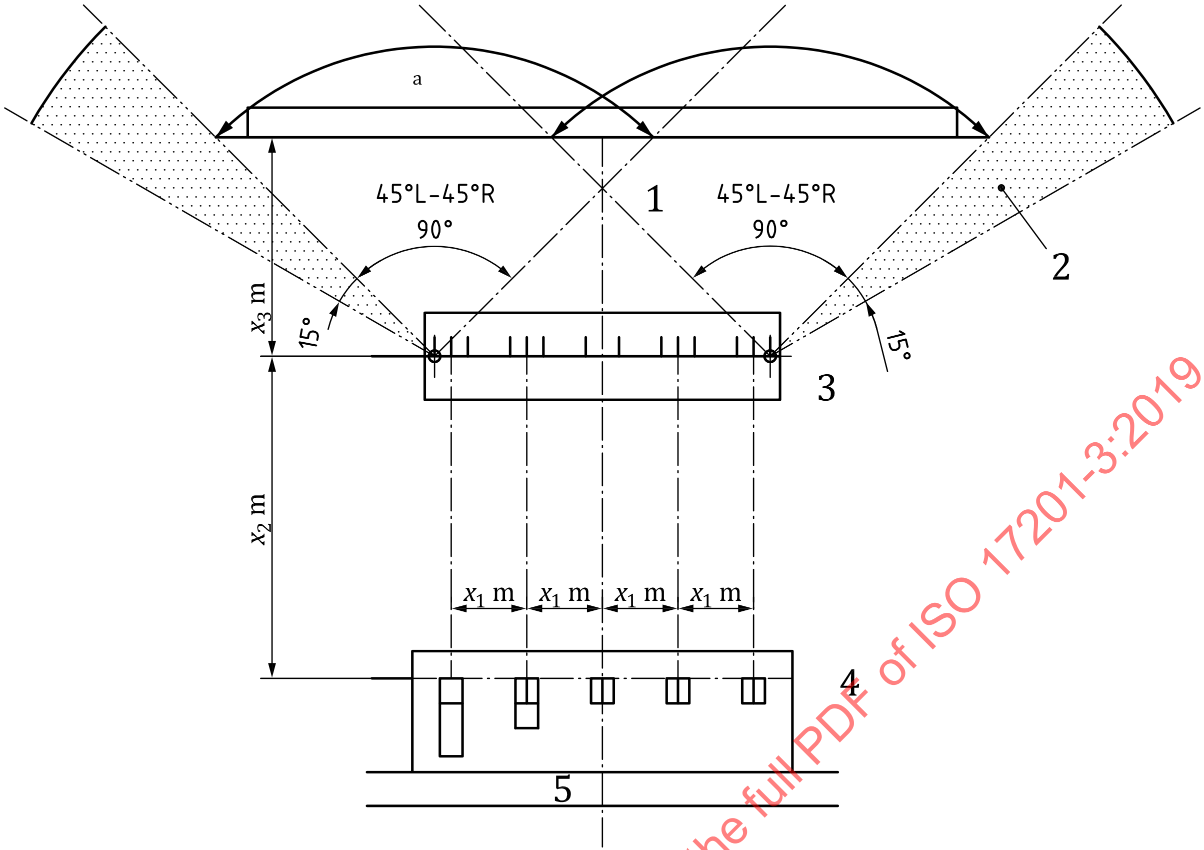

Key

1 firing zone

2 unsafe area

3 launchers line

4 shooter´s positions

5 shooter´s circulation

NOTE The figure is adapted from Reference [26].

a Maximum angle for target launching.

Figure C.3 — Description of firing positions for Olympic trap shooting

Dimensions in metres

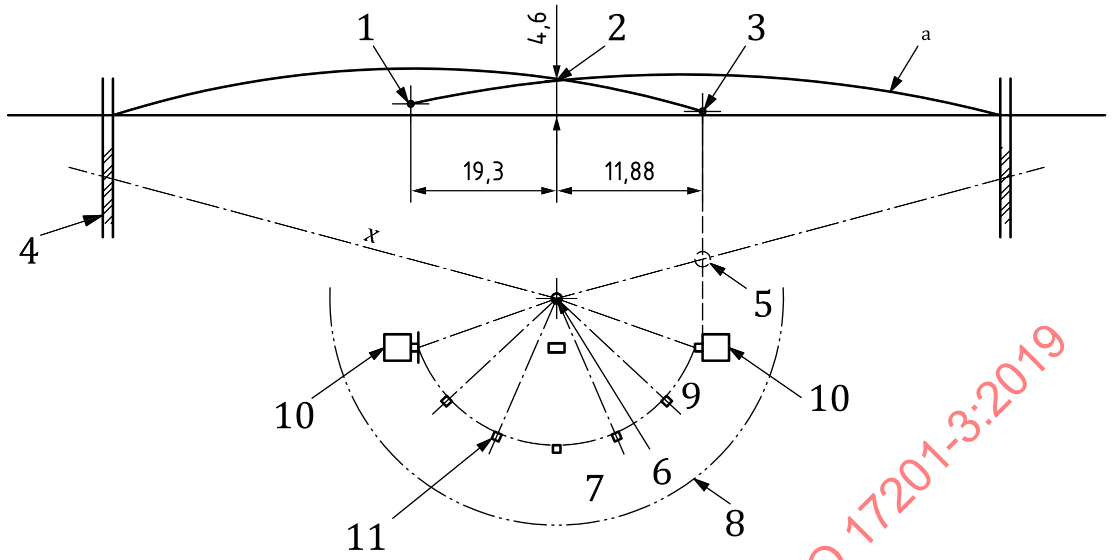

Key

1 pull hut
2 check point
3 mark hut
4 target falling
5 shooting limit pole
6 trajectories check point
7 protection zone
8 public access zone
9 shooter's circle
10 launcher
11 firing position
a Trajectory.

Figure C.4 — Description of firing positions for skeet shooting

In the following example for a skeet range as depicted in Figure C.2, one shooting position is considered. The shooting direction of the range is directly north (*y* direction, *x* direction east, the origin of the co-ordinate system is in front of the shooter in the middle of clay target machines). It has five shooting positions as depicted in Figure C.2.

The first neighbour lives 1 200 m to the east, the second at 500 m to the south from the origin position of the range (see Figure C.2). The different shooting directions have to be taken into account for the angle between the line of fire and the direction to the sites. It is assumed that, for one shooting position, three horizontal (−45°, 0°, 50°) and three vertical (0°, 22,5°, 45°) directions are sufficient, which means that nine different calculations have to be performed.

In the following, the calculation of the sound exposure level produced by the far left shooter (−6 m, −2 m, 1,6 m) is given. The origin of the co-ordinates is shown in Figure C.4 in the middle and in front of the five firing positions. The shooting direction is north, x directs to east and y to north. For site 1, the directivity is accounted for using nine shooting directions.

This leads to the angels between the line of fire and north direction for the left shooting position listed in Table C.1.

Table C.1 — Angles between the line of fire and north direction

Vertical	0,0°	22,5°	45,0°
Horizontal	−45,0°	0°	50,0°

The sound source energy of the shotgun is given in Table C.2.

Table C.2 — Sound source energy level of the shotgun

Frequency	Hz	31,5	63	125	250	500	1 000	2 000	4 000	8 000	16 000
Source energy level	dB	143,8	139,8	138,3	136,9	134,0	130,8	127,6	125,7	126,6	129,9

The directivity is obtained using Table C.3.

Table C.3 — Angular source energy distribution level and the multi pole coefficients to describe the directivity

f	L_q [a]	**Fourier coefficients**												
Hz	dB	0	1	2	3	4	5	6	7	8	9	10	11	12
31,5	104,40	143,8	10,72	1,39	1,25	−0,37	0,18	0,10	0,15	0,12	0,13	0,14	0,10	0,12
63	113,60	139,8	10,04	1,33	0,89	0,04	0,14	−0,08	0,04	0,03	0,02	0,03	0,01	0,02
125	122,20	138,3	10,38	0,82	−0,01	−0,23	−0,26	−0,36	−0,28	−0,25	−0,24	−0,20	−0,20	−0,19
250	128,30	136,9	10,45	2,27	−0,11	−0,74	0,41	−0,30	0,70	0,75	0,72	0,72	0,64	0,66
500	130,80	134,0	10,29	1,51	0,65	0,25	-1,42	−0,44	0,37	0,94	0,98	0,87	0,84	0,80
1 000	130,80	130,8	10,61	2,49	1,36	1,31	−0,76	0,20	−0,03	0,23	0,24	0,15	0,19	0,13
2 000	128,80	127,6	9,32	2,10	0,78	1,27	0,07	0,95	0,38	0,43	0,41	0,32	0,34	0,29
4 000	126,70	125,7	8,83	1,65	1,73	0,94	0,18	1,66	0,49	0,44	0,45	0,34	0,36	0,31
8 000	125,50	126,6	8,50	1,48	1,95	1,48	0,38	1,48	0,31	0,22	0,20	0,11	0,14	0,09
16 000	123,30	129,9	8,60	1,24	1,97	1,00	0,46	1,28	0,28	0,16	0,15	0,08	0,10	0,07

NOTE The shot gun is 609,6 mm (24´´) and the muzzle speed is 400 m/s.

[a] A-weighted.

C.2.2 Free-field shooting range — First site

The coordinate system is depicted in Figure C.4. The origin is 6 m in front of the shooter. The shooter considered has the far left position. Data for various scenarios are presented in Tables C.4 to C.12.

Table C.4 — Reception site 1; shooter: P(−6 m, −2 m, 1,6 m); reception point: P(500 m, 0 m, 5 m); muzzle: P(−6,5 m, −1,5 m, 1,6 m); angle: 134,8°

Frequency	Hz	31,5	63	125	250	500	1 000	2 000	4 000	8 000	16 000
Source energy level	dB	143,8	139,8	138,3	136,9	134,0	130,8	127,6	125,7	126,6	129,9
Directivity (134,8°)	dB	10,0	9,7	10,9	10,9	12,5	12,1	10,0	8,4	8,1	7,6
A_{div} (507 m)	dB	65,1									
A_{air}	dB	0,0	0,1	0,2	0,5	1,0	1,9	4,9	16,6	59,3	88,6
A_{gr}	dB	1,6									
L_E at reception point	dB	67,1	63,4	60,5	58,8	53,8	50,2	46,0	34,1	−7,4	−33,0
$L_{E,A}$ at reception point	dB	56,2									

A_{gr} is calculated according to ISO 9613-2:1996, 7.3.2.

Table C.5 — Reception site 1; shooting direction horizontal: −45° vertical: 22,5° relative to north; shooter: P(−6 m, −2 m, 1,6 m); reception point: P(500 m, 0 m, 5 m); muzzle: P(−6,5 m, −1,5 m, 1,9 m); angle: 130,9°

Frequency	Hz	31,5	63	125	250	500	1 000	2 000	4 000	8 000	16 000
Source energy level	dB	143,8	139,8	138,3	136,9	134,0	130,8	127,6	125,7	126,6	129,9
Directivity (130,9°)	dB	9,6	9,4	10,6	10,9	11,6	11,3	9,3	7,2	7,1	6,7
A_{div} (507 m)	dB	65,1									
A_{air}	dB	0,0	0,1	0,2	0,5	1,0	1,9	4,9	16,6	59,3	88,6
A_{gr}	dB	1,6									
L_E at reception point	dB	67,6	63,7	60,8	58,8	54,7	51,0	46,8	35,2	−6,4	−32,1
$L_{E,A}$ at reception point	dB	56,8									

Table C.6 — Reception site 1; shooting direction horizontal: −45°; vertical: 45,0° relative to north; shooter: P(−6 m, −2 m, 1,6 m); reception point: P(500 m, 0 m, 5 m); muzzle: P(−6,5 m, −1,5 m, 2,1 m); angle: 124,8°

Frequency	Hz	31,5	63	125	250	500	1 000	2 000	4 000	8 000	16 000
Source energy level	dB	143,8	139,8	138,3	136,9	134,0	130,8	127,6	125,7	126,6	129,9
Directivity (124,8°)	dB	8,8	8,8	10,1	10,7	10,0	10,0	8,1	5,6	5,6	5,4
A_{div} (507 m)	dB	65,1									
A_{air}	dB	0,0	0,1	0,2	0,5	1,0	1,9	4,9	16,6	59,3	88,6
A_{gr}	dB	1,6									
L_E at reception point	dB	68,3	64,3	61,3	59,0	56,3	52,3	48,0	36,9	−4,9	−30,8
$L_{E,A}$ at reception point	dB	57,9									

Table C.7 — Reception site 1; shooting direction horizontal: 0,0°; vertical: 0,0° relative to north; shooter: P(−6 m, −2 m, 1,6 m); reception point: P(500 m, 0 m, 5 m); muzzle: P(−6,0 m, −1,3 m, 1,6 m); angle: 89,8°

Frequency	Hz	31,5	63	125	250	500	1 000	2 000	4 000	8 000	16 000
Source energy level	dB	143,8	139,8	138,3	136,9	134,0	130,8	127,6	125,7	126,6	129,9
Directivity (89,8°)	dB	5,5	4,4	4,7	6,0	4,2	5,0	4,0	4,3	3,4	3,5
A_{div} (506 m)	dB	65,1									
A_{air}	dB	0,0	0,1	0,2	0,5	1,0	1,9	4,9	16,6	59,2	88,6
A_{gr}	dB	1,6									
L_E at reception point	dB	71,7	68,7	66,7	63,7	62,1	57,3	52,1	38,2	−2,7	−28,8
$L_{E,A}$ at reception point	dB	63,0									

Table C.8 — Reception site 1; shooting direction horizontal: 0,0°; vertical: 22,5° relative to north; shooter: P(−6 m, −2 m, 1,6 m); reception point: P(500 m, 0 m, 5 m); muzzle: P(−6,0 m, −1,3 m, 1,9 m); angle: 89,7°

Frequency	dB	31,5	63	125	250	500	1 000	2 000	4 000	8 000	16 000
Source energy level	dB	143,8	139,8	138,3	136,9	134,0	130,8	127,6	125,7	126,6	129,9
Directivity (89,7°)	dB	5,4	4,4	4,7	6,0	4,2	5,0	4,0	4,3	3,4	3,5
A_{div} (506 m)	dB	65,1									
A_{air}	dB	0,0	0,1	0,2	0,5	1,0	1,9	4,9	16,6	59,2	88,6
A_{gr}	dB	1,6									
L_E at reception point	dB	71,7	68,7	66,8	63,7	62,2	57,3	52,1	38,2	−2,7	−28,8
$L_{E,A}$ at reception point	dB	63,0									

Table C.9 — Reception site 1; shooting direction horizontal: 0,0°; vertical: 45,0° relative to north; shooter: P(−6 m, −2 m, 1,6 m); reception point: P(500 m, 0 m, 5 m); muzzle: P(−6,0 m, −1,3 m, 2,1 m); angle: 89,6°

Frequency	Hz	31,5	63	125	250	500	1 000	2 000	4 000	8 000	16 000
Source energy level	dB	143,8	139,8	138,3	136,9	134,0	130,8	127,6	125,7	126,6	129,9
Directivity (89,6°)	dB	5,4	4,4	4,7	6,0	4,2	5,0	4,0	4,3	3,4	3,5
A_{div} (506 m)	dB	65,1									
A_{air}	dB	0,0	0,1	0,2	0,5	1,0	1,9	4,9	16,6	59,2	88,6
A_{gr}	dB	1,6									
L_E at reception point	dB	71,7	68,7	66,8	63,7	62,2	57,3	52,1	38,2	−2,6	−28,8
$L_{E,A}$ at reception point	dB	63,0									

Table C.10 — Reception site 1; shooting direction horizontal: 55° vertical: 0,0° relative to north; shooter: P(−6 m, −2 m, 1,6 m); reception point: P(500 m, 0 m, 5 m); muzzle: P(−5,4 m, −1,6 m, 1,6 m); angle: 34,8°

Frequency	Hz	31,5	63	125	250	500	1 000	2 000	4 000	8 000	16 000
Source energy level	dB	143,8	139,8	138,3	136,9	134,0	130,8	127,6	125,7	126,6	129,9
Directivity (34,8°)	dB	−5,6	−5,2	−5,2	−7,7	−8,9	−5,6	−4,6	−3,7	−2,4	−2,7
A_{div} (505 m)	dB	65,1									
A_{air}	dB	0,0	0,1	0,2	0,5	1,0	1,8	4,9	16,6	59,1	88,4
A_{gr}	dB	1,6									
L_E at reception point	dB	82,7	78,3	76,6	77,5	75,2	67,9	60,7	46,2	3,2	−22,5
$L_{E,A}$ at reception point	dB	75,2									

Table C.11 — Reception site 1; shooting direction horizontal: 55° vertical: 22,5° relative to north; shooter: P(−6 m, −2 m, 1,6 m); reception point: P(500 m, 0 m, 5 m); muzzle: P(−5,4 m, −1,6 m, 1,9 m); angle: 39,7°

Frequency	Hz	31,5	63	125	250	500	1 000	2 000	4 000	8 000	16 000
Source energy level	dB	143,8	139,8	138,3	136,9	134,0	130,8	127,6	125,7	126,6	129,9
Directivity (39,7°)	dB	−4,6	−4,2	−4,4	−6,7	−7,2	−4,0	−3,8	−3,1	−1,7	−2,0
A_{div} (505 m)	dB	65,1									
A_{air}	dB	0,0	0,1	0,2	0,5	1,0	1,8	4,9	16,6	59,1	88,4
A_{gr}	dB	1,6									
L_E at reception point	dB	81,8	77,3	75,8	76,5	73,6	66,3	59,9	45,6	2,5	−23,1
$L_{E,A}$ at reception point	dB	73,8									

Table C.12 — Reception site 1; shooting direction horizontal: 55°; vertical: 45,0° relative to north; shooter: P(−6 m, −2 m, 1,6 m); reception point: P(500 m, 0 m, 5 m); muzzle: P(−5,4 m, -1,6 m, 2,1 m); angle: 47,6°

Frequency	Hz	31,5	63	125	250	500	1 000	2 000	4 000	8 000	16 000
Source energy level	dB	143,8	139,8	138,3	136,9	134,0	130,8	127,6	125,7	126,6	129,9
Directivity (47,6°)	dB	−2,7	−2,6	−3,2	−3,4	−2,1	−1,1	−2,0	−1,8	−0,9	−1,3
A_{div} (505 m)	dB	65,1									
A_{air}	dB	0,0	0,1	0,2	0,5	1,0	1,8	4,9	16,6	59,1	88,4
A_{gr}	dB	1,6									
L_E at reception point	dB	79,9	75,7	74,7	73,2	68,5	63,4	58,1	44,3	1,8	−23,8
$L_{E,A}$ at reception point	dB	70,1									

Due to the fact that all nine shooting directions occur with the same probability, the A-weighted equivalent sound exposure level, L_E, for this shooter position is 69,2 dB.

C.2.3 Free-field shooting range — Second site

Similarly to C.2.2, one obtains the data presented in Tables C.13 to C.21 for a second site.

Table C.13 — Reception site 2; shooting direction horizontal: −45°; vertical: 0,0°; relative to north; shooter: P(−6 m, −2 m, 1,6 m); reception point: P(0 m, −600 m, 6 m); muzzle: P(−6,5 m, −1,5 m, 1,6 m); angle: 135,6°

Frequency	Hz	31,5	63	125	250	500	1 000	2 000	4 000	8 000	16 000
Source energy level	dB	143,8	139,8	138,3	136,9	134,0	130,8	127,6	125,7	126,6	129,9
Directivity (135,6°)	dB	10,1	9,8	11,0	10,9	12,6	12,3	10,2	8,6	8,3	7,8
A_{div} (599 m)	dB	66,5									
A_{air}	dB	0,0	0,1	0,2	0,6	1,2	2,2	5,8	19,6	70,0	104,8
A_{gr}	dB	1,6									
L_E at reception point	dB	65,5	61,8	58,9	57,3	52,1	48,2	43,5	29,4	−19,8	−50,8
$L_{E,A}$ at reception point	dB	54,3									

Table C.14 — Reception site 2; shooting direction horizontal: −45° vertical: 22,5° relative to north; shooter: P(−6 m, −2 m, 1,6 m); reception point: P(0 m, −600 m, 6 m); muzzle: P(−6,5 m, −1,5 m, 1,9 m); angle: 131,6°

Frequency	Hz	31,5	63	125	250	500	1 000	2 000	4 000	8 000	16 000
Source energy level	dB	143,8	139,8	138,3	136,9	134,0	130,8	127,6	125,7	126,6	129,9
Directivity (131,6°)	dB	9,6	9,4	10,7	11,0	11,8	11,5	9,4	7,4	7,3	6,9
A_{div} (599 m)	dB	66,5									
A_{air}	dB	0,0	0,1	0,2	0,6	1,2	2,2	5,8	19,6	70,0	104,8
A_{gr}	dB	1,6									
L_E at reception point	dB	66,0	62,2	59,3	57,2	52,9	49,0	44,3	30,5	−18,8	−49,8
$L_{E,A}$ at reception point	dB	54,9									

Table C.15 — Reception site 2; shooting direction horizontal: −45°; vertical: 45,0° relative to north; shooter: P(−6 m, −2 m, 1,6 m); reception point: P(0 m, −600 m, 6 m); muzzle: P(−6,5 m, −1,5 m, 2,1 m); angle: 125,4°

Frequency	Hz	31,5	63	125	250	500	1 000	2 000	4 000	8 000	16 000
Source energy level	dB	143,8	139,8	138,3	136,9	134,0	130,8	127,6	125,7	126,6	129,9
Directivity (125,4°)	dB	8,9	8,8	10,2	10,8	10,2	10,1	8,2	5,7	5,7	5,5
A_{div} (599 m)	dB	66,5									
A_{air}	dB	0,0	0,1	0,2	0,6	1,2	2,2	5,8	19,6	70,0	104,8
A_{gr}	dB	1,6									
L_E at reception point	dB	66,8	62,8	59,8	57,	54,6	50,4	45,5	32,3	−17,2	−48,5
$L_{E,A}$ at reception point	dB	56,0									

Table C.16 — Reception site 2; shooting direction horizontal: 0,0°; vertical: 0,0° relative to north; shooter: P(−6 m, −2 m, 1,6 m); reception point: P(0 m, −600 m, 6 m); muzzle: P(−6,0 m, −1,3 m, 1,6 m); angle: 179,3°

Frequency	Hz	31,5	63	125	250	500	1 000	2 000	4 000	8 000	16 000
Source energy level	dB	143,8	139,8	138,3	136,9	134,0	130,8	127,6	125,7	126,6	129,9
Directivity (179,3°)	dB	14,7	13,0	13,6	13,5	12,0	11,0	8,6	9,0	8,8	9,9
A_{div} (599 m)	dB	66,5									
A_{air}	dB	0,0	0,1	0,2	0,6	1,2	2,2	5,8	19,6	70,1	104,8
A_{gr}	dB	1,6									
L_E at reception point	dB	60,9	58,6	56,3	54,7	52,7	49,5	45,1	28,9	−20,3	−52,9
$L_{E,A}$ at reception point	dB	54,4									

Table C.17 — Reception site 2; shooting direction horizontal: 0,0°; vertical: 22,5° relative to north; shooter: P(−6 m, −2 m, 1,6 m); reception point: P(0 m, −600 m, 6 m); muzzle: P(−6,0 m, −1,3 m, 1,9 m); angle: 158,6°

Frequency	Hz	31,5	63	125	250	500	1 000	2 000	4 000	8 000	16 000
Source energy level	dB	143,8	139,8	138,3	136,9	134,0	130,8	127,6	125,7	126,6	129,9
Directivity (158,6°)	dB	13,2	11,9	12,9	11,6	13,2	12,8	10,4	10,7	10,3	10,5
A_{div} (599 m)	dB	66,5									
A_{air}	dB	0,0	0,1	0,2	0,6	1,2	2,2	5,8	19,6	70,1	104,8
A_{gr}	dB	1,6									
L_E at reception point	dB	62,4	59,7	57,1	56,5	51,5	47,7	43,3	27,3	−21,9	−53,5
$L_{E,A}$ at reception point	dB	53,7									

Table C.18 — Reception site 2; shooting direction horizontal: 0,0°; vertical: 45,0° relative to north; shooter: P(−6 m, −2 m, 1,6 m); reception point: P(0 m, −600 m, 6 m); muzzle: P(−6,0 m, −1,3 m, 2,1 m); angle: 144,3°

Frequency	Hz	31,5	63	125	250	500	1 000	2 000	4 000	8 000	16 000
Source energy level	dB	143,8	139,8	138,3	136,9	134,0	130,8	127,6	125,7	126,6	129,9
Directivity (144,3°)	dB	11,1	10,5	11,9	10,3	13,1	13,4	11,0	10,3	10,0	9,5
A_{div} (599 m)	dB	66,5									
A_{air}	dB	0,0	0,1	0,2	0,6	1,2	2,2	5,8	19,6	70,1	104,8
A_{gr}	dB	1,6									
L_E at reception point	dB	64,5	61,1	58,1	57,9	51,6	47,1	42,7	27,7	−21,6	−52,5
$L_{E,A}$ at reception point	dB	54,0									

Table C.19 — Reception site 2; shooting direction horizontal: 55°; vertical: 0,0° relative to north; shooter: P(−6 m, −2 m, 1,6 m); reception point: P(0 m, −600 m, 6 m); muzzle: P(−5,4 m, −1,6 m, 1,6 m); angle: 124,4°

Frequency	Hz	31,5	63	125	250	500	1 000	2 000	4 000	8 000	16 000
Source energy level	dB	143,8	139,8	138,3	136,9	134,0	130,8	127,6	125,7	126,6	129,9
Directivity (124,4°)	dB	8,8	8,7	10,1	10,7	9,9	9,9	8,0	5,5	5,5	5,3
A_{div} (598 m)	dB	66,5									
A_{air}	dB	0,0	0,1	0,2	0,6	1,2	2,2	5,8	19,6	70,0	104,7
A_{gr}	dB	1,6									
L_E at reception point	dB	66,9	62,9	59,9	57,4	54,8	50,6	45,7	32,5	−17,1	−48,3
Opy of $L_{E,A}$ at reception point	dB	56,2									

Table C.20 — Reception site 2; shooting direction horizontal: 55°; vertical.: 22,5° relative to north; shooter: P(−6 m, −2 m, 1,6 m); reception point: P(0 m, −600 m, 6 m); muzzle: P(−5,4 m, −1,6 m, 1,9 m); angle: 121,7°

Frequency	Hz	31,5	63	125	250	500	1 000	2 000	4 000	8 000	16 000
Source energy level	dB	143,8	139,8	138,3	136,9	134,0	130,8	127,6	125,7	126,6	129,9
Directivity (121,7°)	dB	8,5	8,4	9,7	10,7	9,4	9,4	7,6	5,0	5,0	4,9
A_{div} (598 m)	dB	66,5									
A_{air}	dB	0,0	0,1	0,2	0,6	1,2	2,2	5,8	19,6	70,0	104,7
A_{gr}	dB	1,6									
L_E at reception point	dB	67,2	63,2	60,2	57,5	55,4	51,2	46,2	33,0	−16,5	−47,8
$L_{E,A}$ at reception point	dB	56,6									

Table C.21 — Reception site 2; shooting direction horizontal: 55°; vertical: 45,0° relative to north; shooter: P(−6 m, −2 m, 1,6 m); reception point: P(0 m, -600 m, 6 m); muzzle: P(−5,4 m, −1,6 m, 2,1 m); angle: 117,2°

Frequency	Hz	31,5	63	125	250	500	1 000	2 000	4 000	8 000	16 000
Source energy level	dB	143,8	139,8	138,3	136,9	134,0	130,8	127,6	125,7	126,6	129,9
Directivity (117,2°)	dB	8,1	8,0	9,1	10,7	8,7	8,6	7,0	4,5	4,4	4,4
A_{div} (598 m)	dB	66,5									
A_{air}	dB	0,0	0,1	0,2	0,6	1,2	2,2	5,8	19,6	70,0	104,7
A_{gr}	dB	1,6									
L_E at reception point	dB	67,6	63,7	60,9	57,5	56,0	52,0	46,7	33,5	−15,9	−47,3
$L_{E,A}$ at reception point	dB	57,2									

Average A-weighted sound exposure level, $L_{E,A}$ for the shooter position: 55,4 dB.

